ผลของการปรับปรุงตัวเร่งปฏิกิริยานิกเกิลบนตัวรองรับเซลลูโลสด้วยอะลูมิเนียมและซิลิคอน สำหรับคาร์บอนไดออกไซด์ไฮโดรจิเนชัน

นางสาวณัฏฐกานต์ จุงจิตตเมต

วิทยานิพนธ์นี้เป็นส่วนหนึ่งของการศึกษาตามหลักสูตรปริญญาวิศวกรรมศาสตรมหาบัณฑิต
สาขาวิชาวิศวกรรมเคมี ภาควิชาวิศวกรรมเคมี
คณะวิศวกรรมศาสตร์ จุฬาลงกรณ์มหาวิทยาลัย
ปีการศึกษา 2556

EFFECT OF ALUMINIUM AND SILICON MODIFICATION ON CELLULOSE-SUPPORTED NICKEL CATALYSTS FOR CARBONDIOXIDE HYDROGENATION

Ms. Nattakan Jungjittamat

A Thesis Submitted in Partial Fulfillment of the Requirements
for the Degree of Master of Engineering Program in Chemical
Engineering Department of Chemical Engineering
Faculty of Engineering
Chulalongkorn University
Academic Year 2013

Thesis Title	EFFECT OF ALUMINIUM AND SILICON MODIFICATION ON CELLULOSE-SUPPORTED NICKEL CATALYSTS FOR CARBONDIOXIDE HYDROGENATION
By	Miss Nattakan Jungjittamat
Field of Study	Chemical Engineering
Thesis Advisor	Associate Professor Bunjerd Jongsomjit, Ph.D.

Accepted by the Faculty of Engineering, Chulalongkorn University in Partial Fulfillment of the Requirements for the Master's Degree

.....Dean of the Faculty of Engineering
(Associate Professor Boonsom Lerdhirunwong, Dr.Ing.)

THESIS COMMITTEE

.....Chairman
(Associate Professor Muenduen Phisalaphong, Ph.D.)

.....Thesis Advisor
(Associate Professor Bunjerd Jongsomjit, Ph.D.)

.....Examiner
(Chutimon Satirapipathkul, Ph.D.)

.....External Examiner
(Ekrachan Chaichana, D.Eng)

ณัฏฐกานต์ จุงจิตตเมต : ผลของการปรับปรุงตัวเร่งปฏิกิริยานิกเกิลบนตัวรองรับเซลลูโลสด้วยอะลูมิเนียมและซิลิคอนสำหรับคาร์บอนไดออกไซด์ไฮโดรจิเนชัน (EFFECT OF ALUMINIUM AND SILICON MODIFICATION ON CELLULOSE-SUPPORTED NICKEL CATALYSTS FOR CARBONDIOXIDE HYDROGENATION) อ. ที่ปรึกษาวิทยานิพนธ์หลัก : รศ. ดร. บรรเจิด จงสมจิตร, 66 หน้า

งานวิจัยนี้ได้ศึกษาคุณลักษณะของตัวเร่งปฏิกิริยาเมื่อปรับปรุงตัวเร่งปฏิกิริยานิกเกิลบนตัวรองรับเซลลูโลสด้วยอะลูมิเนียมและซิลิคอนสำหรับคาร์บอนไดออกไซด์ไฮโดรจิเนชัน โดยใช้วิธีการเคลือบฝังแบบเปียกในการเตรียมตัวเร่งปฏิกิริยา ตัวเร่งปฏิกิริยานิกเกิล 20 % โดยน้ำหนักบนตัวรองรับเซลลูโลสที่ถูกปรับปรุงด้วยซิลิกอนและอะลูมิเนียม 2, 6, 12 % โดยน้ำหนักจะถูกนำไปอบที่อุณหภูมิ 100 องศาเซลเซียสเป็นเวลา 24 ชั่วโมง จากนั้นนำไปเผาในอากาศที่อุณหภูมิ 200 องศาเซลเซียส ความดัน 1 บรรยากาศเป็นเวลา 5 ชั่วโมง หลังจากนั้นนำตัวเร่งปฏิกิริยาที่ได้ไปทำการศึกษาคุณลักษณะด้วยวิธีต่างๆ เช่น การถ่ายภาพจากกล้องจุลทรรศน์อิเล็คตรอนแบบส่องกราด, การวิเคราะห์เฟสด้วยวิธีการกระเจิงรังสีเอ็กซ์, การดูดซับทางกายภาพของแก๊สไนโตรเจนและการวิเคราะห์โดยความร้อน ผลที่ได้จากการทดลองพบว่าการเปลี่ยนแปลงของแก๊สคาร์บอนไดออกไซด์และอัตราการเกิดปฏิกิริยามีแนวโน้มเพิ่มมากขึ้นเมื่อมีการปรับปรุงตัวรองรับโดยใช้อะลูมิเนียม เมื่อใส่อะลูมิเนียม 6 % โดยน้ำหนักเพื่อปรับปรุงตัวรองรับพบว่าค่าการเปลี่ยนแปลงของแก๊สคาร์บอนไดออกไซด์มากที่สุดเท่ากับ 99.51 % และอัตราการเกิดปฏิกิริยามากที่สุดเท่ากับ 63.98 $gCH_2/gcat.hr$ ในส่วนของค่าการเลือกเกิดมีเทน ซิลิกอนเป็นปัจจัยที่สำคัญมากที่ส่งผลในการปรับปรุงค่าการเลือกเกิด และความเสถียรเชิงอุณหภูมิของตัวเร่งปฏิกิริยา จากการทดลองที่ได้ค่าการเลือกเกิดจะมีค่ามากที่สุดเท่ากับ 83.57 % เมื่อใส่ซิลิกอน 2 % โดยน้ำหนักเพื่อปรับปรุงตัวรองรับ

ภาควิชา……..วิศวกรรมเคมี ลายมือชื่อนิสิต……..……..

สาขาวิชา……วิศวกรรมเคมี……. ลายมือชื่ออ.ที่ปรึกษาวิทยานิพนธ์หลัก……...……....

ปีการศึกษา…….2556……..

##5470928721: MAJOR CHEMICAL ENGINEERING
KEYWORDS: CELLULOSE/ ALUMINIUM/ SILICON / NICKEL CATALYST/ CARBON DIOXIDE HYDROGENATION

NATTAKAN JUNGJITTAMAT: EFFECT OF ALUMINIUM AND SILICON MODIFICATION ON CELLULOSE-SUPPORTED NICKEL CATALYSTS FOR CARBONDIOXIDE HYDROGENATION. ADVISOR: ASSOC. PROF. BUNJERD JONGSOMJIT, Ph.D., 66 pp.

The catalytic performances of aluminium and silicon modification on cellulose-supported nickel catalyst for CO_2 hydrogenation were studied. The catalysts were prepared by the incipient wetness impregnation method. Nickel (20 wt%) was impregnated onto the aluminium modification (2, 6 and 12 wt%) and silicon modification (2, 6 and 12 wt%) of Avicel and dried at 100°C for 24 hr. Then, the samples were calcined under air condition at 200°C for 24 hr. CO_2 hydrogenation was carried out at 220°C and 1 atm for 5 hr. The catalysts were characterized by SEM, EDX, XRD, BET and TGA. The experimental results showed that CO_2 conversion and rate of reaction were improved when using aluminium loading on the support. The highest CO_2 conversion (99.51 %) and rate of reaction (63.98 gCH_2/gcat.hr) were obtained when using alumina loading of 6 wt%. In case of selectivity, silicon had important effect to improve selectivity and thermal stability of catalysts. The maximum selectivity (83.57 %) was reached over 2 wt% of silicon.

Department : ……Chemical Engineering…. Student's Signature…….

Field of Study : …Chemical Engineering…. Advisor's Signature……...…….

Academic Year : …..2013…….

ACKNOWLEDGEMENTS

I would not have been possible to complete my thesis without help, support, guidance and encouragement of my advisor, committee members, teachers, friends, science team and family.

Foremost, I would like to express my sincere gratitude to Asst. Prof. Dr. Bunjerd Jongsomjit, my advisor, for his guidance and his support for all the time of research and writing of this thesis. Also, I'd like to thank for giving me an opportunity to be a part of catalyst researchers. The author would like to thanks Thailand Research Fund (TFR) for supporting me.

I would like to thank Parichat Thipayang, Salisa Pungsuk, Pisut Sukkasem, Piyaporn Harinputtasil, Kotchasak Yupapornopa and Chanidapa Padungpitakchon who are my best friends. They were always willing to help and give their best suggestions and motivations.

Finally, I would like to thank my family. They always support me and encourage me with their best wishes.

CONTENTS

Page

Page

CHAPTER

LIST OF TABLES

Page

LIST OF FIGURES

Page

Page

CHAPTER I

INTRODUCTION

Introduction

In these days, carbondioxide (CO_2) is one of major drivers, which is bringing the world into global warming and its chain effects. CO_2 is the major component of green house gas and causes of climate change. Most of CO_2 in the Earth's atmosphere is emitted from human activities. The main human activity that emits CO_2 is the combustion of fossil fuels for transportation. From the historical, the concentration of CO_2 in the atmosphere tends to increase from decade to decade. Hydrogenation of CO_2 is an important reaction in aspects of global environmental protection and utilization of carbon sources of syntheses hydrocarbons [1]. Hydrogenation of CO_2 to chemical feedstocks has been paying much attention to transform CO_2 to commercial chemicals. Consequently, CO_2 is actually a valuable carbon resource, which can transform into other chemical components such as hydrocarbon, alcohols, carboxylic acids and light olefins [2].

Hydrogenation is a chemical reaction, which inserts hydrogen molecule (H_2) to unsaturated compound. Normally, this reaction takes place in high temperature, high pressure and highly exothermic reaction. So catalyst is considered in hydrogenation to reduce operating temperature, operating pressure and increase productivity.

Nickel catalysts are preferred to use in hydrogenation and generally prepared by the incipient wetness impregnation, ion exchange and precipitation. Incipient wetness impregnation is the simplest method for synthesis catalyst. The dominate properties of nickel are high activity, selectivity and easy to reduce [3]. The disadvantage is formation of Ni by sintering and coke, which will decrease catalyst properties [4].

Avicel PH101 is one of commercial microcrystalline cellulose, not dilute in acid or common organic solvent and not dissolve in water. The appearances are white

or quasi-white powder and odorless. It often utilizes in medical processing, especially to improve the quality of pellets in extrusion–spheronization process [5]. Furthermore, it is developed to biomass or biofuel production in the name of cellulosic biofuels [6]. Nevertheless, it is abundant of cellulose to synthesize as catalyst for fuel production, such as CO_2 hydrogenation. Due to microcrystalline structure property and non dissolve in common organic solvent, it is the attractive point to investigate Avicel PH101 as catalyst support in CO_2 hydrogenation.

In this research, carbon dioxide hydrogenation to methane is studied over Ni/Avicel PH101. The effect of the promoter (Al and Si) to improve the characteristics of catalyst and conversion is investigated.

Motivation

Ni/Avicel PH101 may be one of effective catalysts for CO_2 hydrogenation, high conversion, high reaction rate and no side reaction, but the disadvantage of cellulose is slightly lower thermal stability. In this research, thermal stability of Avicel PH101 may be improved by promoter (Al and Si). Al and Si are the major metal to improve thermal stability as promoter in catalytic research. In this work, thermal stability of catalyst was investigated by modified support with Al and Si for CO_2 hydrogenation.

Objective of the study

To investigate the effect of modified support with Al and Si on Ni/Avicel PH101 in CO_2 hydrogenation and characterization of catalyst.

Scope and the limitation of the study

Part 1: To investigate Ni/Avicel PH101 in CO_2 hydrogenation

- Loading of Ni (20 wt%) on Avicel PH101 by impregnation method.
- Dry catalyst precursor at 100°C for 24 hr.
- Calcine in air at 200°C for 4 hr.

- Characterization of catalyst precursor by SEM, EDX, XRD, TGA and BET.
- Study the activity and selectivity of catalyst precursor on CO_2 hydrogenation at 220°C, 1 atm for 5 hr.

Part 2: To investigate the effect of modified support with Al on Ni/Avicel PH101 in CO_2 hydrogenation

- Preparation of modified support with Al (2, 6, 12 wt% loading) via impregnation method.
- Dry catalyst precursor at 100°C for 24 hr.
- Calcine in air at 200°C for 4 hr.
- Loading of Ni (20 wt%) on Avicel PH101 by impregnation method.
- Dry catalyst precursor at 100°C for 24 hr.
- Calcine in air at 200°C for 24 hr.
- Characterization of catalyst precursor N_2 physisorption, SEM, XRD, TGA.
- Study the activity and selectivity of catalyst precursor on CO_2 hydrogenation at 220°C, 1 atm for 5 hr.

Part 3: To investigate the effect of modified support with Si on Ni/Avicel PH101 in CO_2 hydrogenation

- Preparation of modified support with Si (2, 6, 12 wt% loading) via impregnation method.
- Dry catalyst precursor at 100°C for 24 hr.
- Calcine in air at 200°C for 4 hr.
- Loading of Ni (20 wt%) on Avicel PH101 by impregnation method.
- Dry catalyst precursor at 100°C for 24 hr.
- Calcine in air at 200°C for 24 hr.
- Characterization of catalyst precursor by N_2 physisorption, SEM, XRD, TGA.

- Study the activity and selectivity of catalyst precursor on CO_2 hydrogenation at 220°C, 1 atm for 5 hr.

Expected results

- To improve thermal stability of Ni/Avicel PH101 by modified catalyst with Al and Si.
- To improve conversion of CO_2 hydrogenation.
- To improve selectivity of CO_2 hydrogenation
- To develop new catalyst from organic support for CO_2 hydrogenation.

Produce national or international research database from knowledge in the experiment.

CHAPTER II

LITERATURE REVIEW

2.1 Nickel

Aksoylu and Onsan [7] reported investigated the effect of Ni/Al_2O_3 on CO and CO_2 hydrogenation at 525K. The coprecipitated Ni/Al_2O_3 (0, 5, 11, 16.5 wt%) and impregnated Ni/Al_2O_3 (0, 5, 10, 15 wt%) were catalyst precursors. The additional metal (Ni) from coprecipitated was effective than impregnated when increase with metal loading. Metal loading in impregnation should be optimum. If metal loading increase more than optimum, metal loading content in catalyst will not increase because metal can't load into support due to pore blockage by immoderate nickel. For CO hydrogenation, the specific activity of coprecipitated was decreased with increase metal loading though specific activity of impregnated increased. In CO_2 hydrogenation, coprecipitated catalysts were higher activity and lower side reaction than impregnated catalyst. The relation of metal loading and specific activity was same as CO hydrogenation.

Li and Lu [8] reported that investigated reaction performance of partial oxidation of methane over Ni/SiO_2 catalysts using monodisperse silica sol as supporting precursor. Silica sol was prepared by ion exchange method. Partial oxidation of methane was carried out in fixed-bed quartz reactor under atmospheric pressure. Ni/SiO_2 showed the excellent reaction performance and high activity during partial oxidation of methane. The best performance for methane partial oxidation was observed when used catalyst with Ni loading of 3.8 wt%. The structure and reducing properties of catalyst were characterized by BET, TPR and XRD. From the characterization methods, the active species of catalyst can fully sustain Ni^0 phase under low reaction temperature in water-rich product mixture.

Nickel catalysts on rice husk ash-alumina ($Ni/RHA\text{-}Al_2O_3$) were prepared by incipient wetness impregnation. The catalysts were investigated by TPR, XPS, XRD, SEM and BET. The samples were tested by CO_2 hydrogenation with H_2/CO_2 ratio of

4:1 for temperature 400-800°C. The XPS analysis of catalyst demonstrated the presence of spinel. The interaction between nickel and support was strong and difficult to reduce compare with one nickel oxide compound. The optimum nickel loading with maximum surface area was 15 wt%, from TRP analysis. The crystallite sizes of supported NiO, CO_2 conversion and CH_4 yield were increased with increase in nickel loading. The reaction temperature of 500°C might be the optimum temperature for CO_2 hydrogenation, maximum selectivity and yield from Feg et al. [3].

2.2 Cellulose

Wada et al. [9] reported studied X-ray diffraction on the thermal expansion behavior of cellulose Iß and its high-temperature phase. Cellulose Iß from algal was prepared by hrdrothermal treatment employing in 0.1 M NaOH solution at 260°C for 30 min. The samples were investigated by using x-ray diffraction from temperature range 20-300°C with heating rate of 5°C/min. The results showed that Cellulose Iß was transformed into higher-temperature phase at temperature more than 230°C. The anisotropic thermal expansion of cellulose Iß in lateral direction is appeared because the crystal structure and hydrogen-bonding system of cellulose. At high temperature phase, the result emphasized that cellulose is composed of a two-chain monoclinic unit cell.

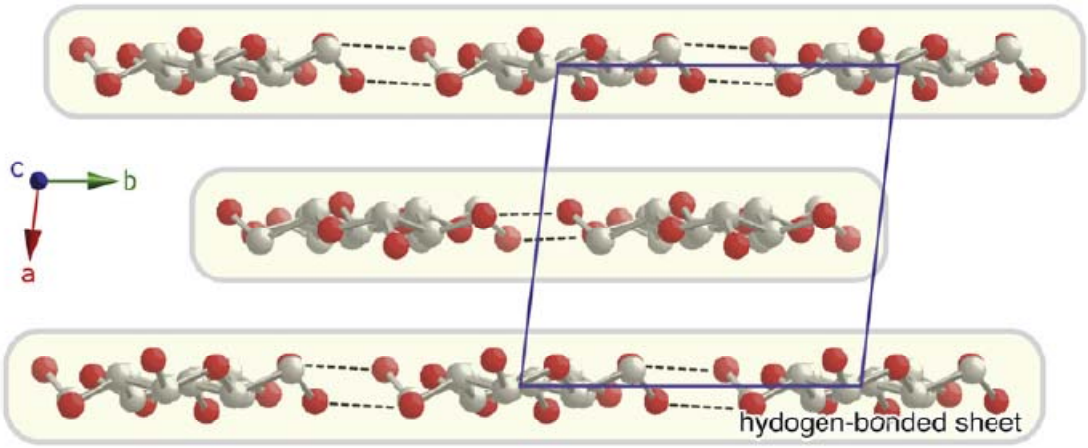

Figure 2.1 Chain arrangement of cellulose Iß

Above figure showed chain arrangement along the view parallel to chain axis and the unit cell of cellulose Iß. The dotted lines orientated almost parallel to the b-axis, represent intermolecular hydrogen bonds. The hydrogen-boned sheets stack through van der Waals interaction to forming of the cellulose Iß crystal.

Cellulosic mantles of tunicate were purified and hydrolyzed into microcrystals with sulfuric acid. Then it was reformed to oriented films. Oriented films were stacked parallel on top with one another up to thickness of 200µm and investigated in this experiment. A set of coordinates for all atoms in cellulose Iß was investigated by x-ray and neutron fiber diffraction. The x-ray data was used to observed carbon and oxygen atom positions. Fourier-difference analysis using neutron diffraction was used to determine hydrogen atom positions. The structure of cellulose consisted of two parallel groups. The hydrogen atoms in the intramolecular O3-O5 hydrogen bonds showed same position but the intramolecular O2-O6 covered slightly difference forms Nishiyama et al. [10].

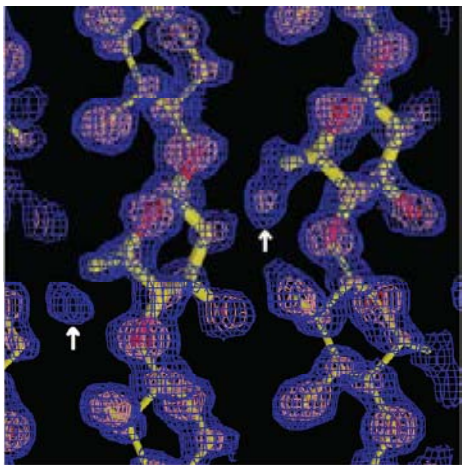

Figure 2.2 The skeletal model.

Above model represents the cellulose chain, which one residue of both the origin and center chains highlighted by thicker lines.

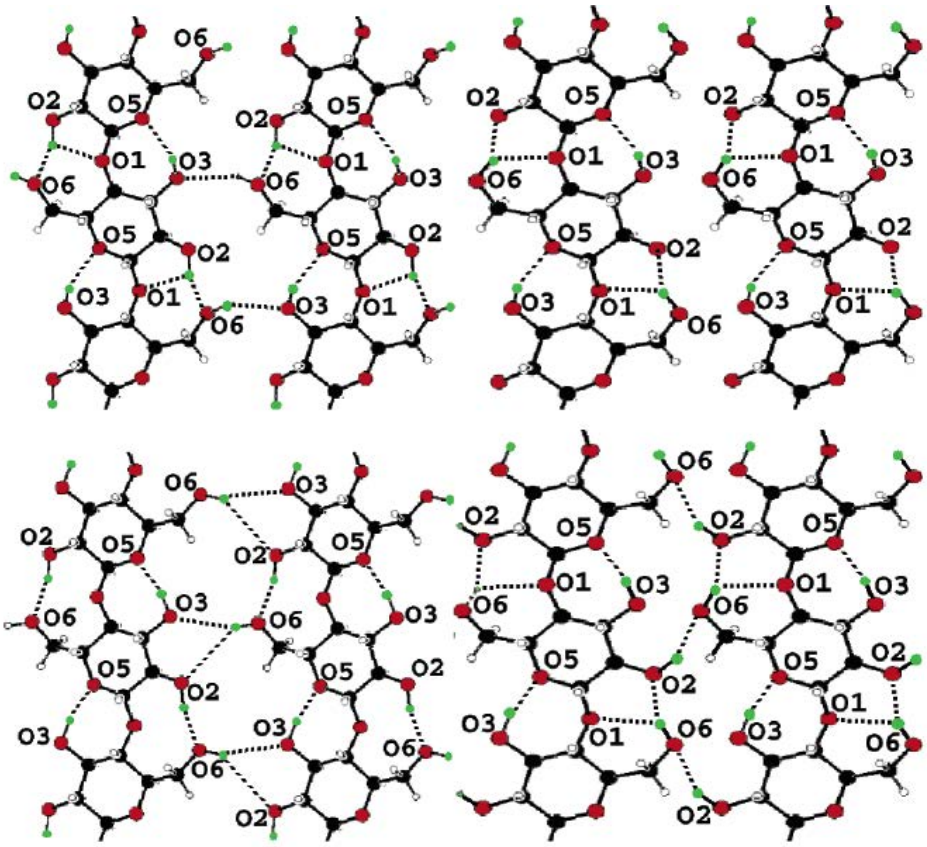

Figure 2.3 Hydrogen bonds of of cellulose Iß

Schematic represents the hydrogen bonds in the origin (top) and center (bottom) sheets of cellulose Iß. Carbon, oxygen, hydrogen and deuterium atoms are colored black ( ), red ( ), white ( ) and green ( ), respectively. Hydrogenbonds are represented by dotted lines. Only the oxygen atoms involved in hydrogen bonding have been labeled for clarity.

2.3 Promoter

Milburn et al. [11] reported that studied promoted iron Fischer-Tropsch catalyst characterization by thermal analysis. Impregnation is used to prepare unpromoted iron oxide by addition of ammonium hydroxide in Fe^{III}nitrate(1M). Modifier tetraethyl Orthosilicate [$Si(OC_2H_5)_4$] and aluminium(III) nitrate [$Al(NO_3)_3$] were prepared by precipitation on iron oxide catalyst. Promoter loading (Si and Al) was 2, 6, 12 wt%. From the experiment, Si was more effective than Al because Si (SiO^-_2) was strongly chemical bond with iron oxide (FeO^+_2) than Al (AlO^-_2). Exotherm temperature of Si was higher than Al. Promoter loading should be suitable and optimum. The Si and Al promoter was no impact to Fischer-Tropsch catalyst selectivity and activity.

Suna et al. [12] reported that improved catalytic activity and stability of mesostructured sulfated zirconia by Al promoter in isomerization of n-butane to isobutene. Al promoted mesostructured sulfated zirconia (Al-MSZ-5) was prepared by triblock polymer surfactant (P123) with ethanol. Conventional sulfated zirconia (SZ) was prepared by immersing dried $Zr(OH_4)$ in 0.5M of $(NH_4)_2SO_4$ for 30 min and calcine at 550°C for 3hr. As a result from TG, Al promoted mesostructured sulfated zirconia was improved thermal stability and activity compare with conventional mesostructure due to crystalline phase of zirconia was difference from preparation method.

Houa et al. [13] reported investigated effect of SiO_2 content on iron-base catalyst for slurry Fischer-Tropsh synthesis to improve the attrition resistance. The $Fe/Cu/K/SiO_2$ catalyst samples were prepared by combination of co-precipitation and spray-dried method. $Fe(NO_3)•9H_2O$ and $Cu(NO_3)$ are used with Fe/Cu weight ratio of

100/5 to precipitating in sodium carbonate solution. SiO_2 sol solution and K_2CO_3 solution were added to precipitate. The catalyst samples (100Fe/5Cu/4.2K/xSiO_2, x=15, 20, 25, 30, 40) were re-slurried, spary-dried and calcination at 400°C for 5 hr. Surface area of catalyst slightly increases with SiO_2 loading, nevertheless, average pore diameter slightly decrease and pore volumes nearly unchanged. In addition, the reducibility was also improved by increasing SiO_2 content. The catalyst stability was improved due to the strongly Fe-SiO_2 intersection. In summary, the result may be difference because of difference preparation method. From FTS, the activity was improved with increase SiO_2 loading. The reasons for support the result are SiO_2 loading increase, K_p and water-gas shift decrease, tend to decrease of CO_2 but partial pressure of H_2O increase so CO_2 product will be raise

.

CHAPTER III

THEORY

3.1 Nickel[14, 15]

Nickel is a transition metals which atomic number 28. It is a silvery white metal, hard and ductile. Normally, nickel appears in combination with sulphur and iron in pentlandite, with sulpher in millerite, with arsenic in the mineral nickeline and with arsenic and sulpher in nickel glance. Nickel is a naturally magnetostrictive material at room temperature. Nickel is widely used in metallurgical process such as alloy product, nickel-cadmium batteries, stainless steel, brasses and bronzes.

The generally active phase in catalyst for CO_2 hydrogenation is nickel (Ni) such as Ni/La_2O_3, Ni/CaO and Ni/Si_2O_3. The significant point of Ni is easily reduced to Ni metal, which is the most active state for hydrogenation. Unfortunately, coke formation happen during reduction period and it effects to nickel dispersion and morphology. The dispersion of nickel will decrease and morphology will change.

The properties of nickel are shown:

Table 3.1 Properties of nickel

Property	Value
Name, symbol	Nickel, Ni
Atomic number	28
Element category	Transition metal
Standard atomic weight	58.69
Melting point, °C	1453
Boiling point, °C	2913
Latent heat of fusion, ΔHfus kJ/mol	17.48
Latent heat of vaporization, ΔHvap kJ/mol	377.5
Specific heat, kJ/(mol.•K) at 25°C	26.07
Atomic radius, pm	124

Property	Value
Crystal structure	Face centered cubic
Magnetic ordering	Ferromagnetic
Thermal conductivity, W/(m•K) at 27 °C	90.9
Brinell hardness, MPa	700

3.2 Cellulose

Avicel PH101 is microcrystalline cellulose (organic compound) which chemical formula is $(C_6H_{10}O_5)_n$. The appearances are white or quasi white, fine crystalline, odorless and tasteless. It does not dissolve in water and common organic solvent but dissolve in acid. They partly dissolve and swell in dilute alkali. Avicel PH101 is the most popular grade for all tableting medical processing, especially for wet granulation and globular granule production. Furthermore, it is a food additive to increase dispersion and agglomeration in food industry as anti-caking agent, dispersant, binder for butter, ice and cold drinks food products. Cellulose shall be stored in sealed container and kept in cool, dark and drying place[9, 10].

Physical and chemical properties of Avicel PH101 are shown:

Table 3.2 Physical and chemical properties of Avicel PH101

Property	Value
Name	Avicel PH101
Chemical formula	$(C_6H_{10}O_5)_n$
PH	5-7 (11% solids dispersion)
Specific gravity (water=1)	0.2-0.5
Solubility in water	Insoluble
Percent volatile	1-5%
Melting point, °C	177-184
Density, g/cm^3	1.5

The typical structure of cellulose as shown:

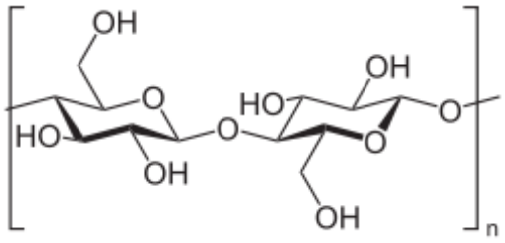

Figure 3.1 Cellulose structure

3.3 Promoter

Silica [13, 16, 17]

Silica is a chemical compound of silicon and oxygen with chemical formula SiO_2. Continuous framework of SiO_4 is made up of sharing oxygen atoms between two tetrahedral. As a result, overall chemical formula is showed SiO_2. Most of silica in natural was performed of sand orquartz and cell walls of diatoms. There are several crystal structures because of difference operating condition in solidification. Only α-quartz is stable under normal condition and common crystalline silicon which found in nature.

Tetrahedral coordination of silica (SiO_2) as shown:

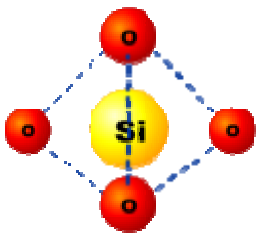

Figure 3.2 Tetrahedral coordination of silica (SiO_2)

α-quartz structure as shown:

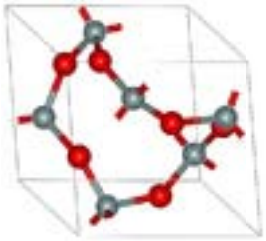

Figure 3.3 α-quartz structure

Silicon dioxide is a very thin film cover on silicon when silicon is contacts to oxygen. Various methods used to synthesis silicon dioxide layer are shown:

- Low temperature oxidation of silane at 400-450°C

$SiH_4 + 2O_2 \longrightarrow SiO_2 + 2H_2O$

- Decomposition of tetraethyl orthosilicate (TEOS) at 680-730°C

$Si(OC_2H_5)_4 \longrightarrow SiO_2 + 2H_2O + 4C_2H_4$

- Plasma enhanced chemical vapor deposition using TEOS at 400°C

$Si(OC_2H_5)_4 + 12O_2 \longrightarrow SiO_2 + 10H_2O + 8CO_2$

- Pyrogenic silica or fume silica synthesis by burning $SiCl_4$ in rich hydrogen and oxygen

$SiCl_4 + 2H_2 + O_2 \longrightarrow SiO_2 + 4HCl$

Normally, silicon is not dissolve into water but it can dissolve into hydrofluoric acid (HF), hydroxide, metal oxide and hot concentrated alkali.

$SiO_2 + 2NaOH \longrightarrow Na_2SiO_3 + H_2O$

In semiconductor industry, hydrofluoric acid (HF) is major chemical solution to remove silica from the production process.

$SiO_2 + 6HF \longrightarrow H_2SiF_6 + 2H_2O$

- The reaction of basic metal oxide and silica can produce commercial glass.

$2NaO + SiO_2 \longrightarrow Na_4SiO_4$

$Na_2O + SiO2 \longrightarrow Na_2SiO_3$

$(0.25\text{-}0.8)Na_2O + SiO_2 \longrightarrow$ glass

Excellent material properties of silica are outstanding from others, in case of high hardness, high thermal stability and high surface area. Because of mesoporous property, silica is commonly used in the field of catalyst, sorption in hygroscopic application and separation. There are several applications of silica such as glass for windows or beverage container, optical fiber for telecommunications, whiteware ceramics and primary component of rice husk ash for cement production. Furthermore, in food industry silica is used for common additive as flow agent in powdered food and absorb water in hygroscopic. In electrical component, it can use for insulator to limit electrical current.

Table 3.3 Physical and chemical properties of silica

Property	Value
Name	Silica or silicon dioxide
Chemical formula	SiO_2
Appearance	Transparent crystals
Density, g/cm^3	2.648
Solubility in water	Insoluble
Melting point, °C	1600-1725
Boiling point, °C	2230
Standard enthalpy of formation, kJ/mol	-911
Standard molar entropy, J/(mol•K)	42

Alumina or aluminiumoxide (Al_2O_3) [18]

Alumina is synthetically produced aluminum oxide (Al_2O_3) or corundum, amphoteric oxide, white or nearly colorless crystalline substance. Corundum is the common form of crystalline alumina. The lowest formation temperature of γ-Al_2O_3 phase is 700-800°C and appear in hexagonal closed-packed structure. It was showed in various transient metastable (chi (χ), kappa (κ), eta (η), theta (θ), delta (δ), and gamma (γ).) phases. Gamma (γ) phase is only one thermodynamically stable phase with high melting point (2047°C) and high hardness (21 GPa). Normally, it is referred to alumina (δ-alumina), aloxide or corundum in its crystalline form.

Activated alumina is a porous, granular substance that is used for catalyst and adsorbent to remove water from liquids and gases. Alumina catalyst is wildly use for industrial catalyst such as dehydrogenation of alcohols to alkenes, hydrodesulfurization and polymerization. Calcined alumina is made to ceramic products, insulators, integrated-circuit packages and sandpaper. Significance properties of alumina are low electric conductivity, resistance to chemical attack, hardness, high strength, thermal insulating, high melting point and high optical transparency. But the low strength and toughness limit for some application such as cutting tool.

Table 3.4 Physical and chemical properties of alumina

Property	Value
Name	Alumina, aluminium oxide or aloxide
Chemical formula	Al_2O_3
Molar mass, g/mol	101.96
Odour	Odourless
Density, g/cm^3	3.95-4.1
Melting point	2072
Boiling point	2977
Solubility in water	Insolubility

Property	Value
Thermal conductivity, W/(m•K)	30
Crystal structure	Trigonal
Standard enthalpy of formation, kJ/mol	-1675.7
Standard molar entropy, kJ/mol	50.92
Flash point	Non-flammable

3.4 CO_2 hydrogenation [19]

Hydrogenation is addition hydrogen molecule (H_2) to pi bond of unsaturated compound. Double bond between carbon atoms in hydrocarbon consists of sigma bond and pi bond. Carbon-carbon pi bond quite weaks compare to sigma bond so hydrogen molecule is adding at pi bond such as alkenes to alkanes or unsaturated fat oil to saturated fat oil.

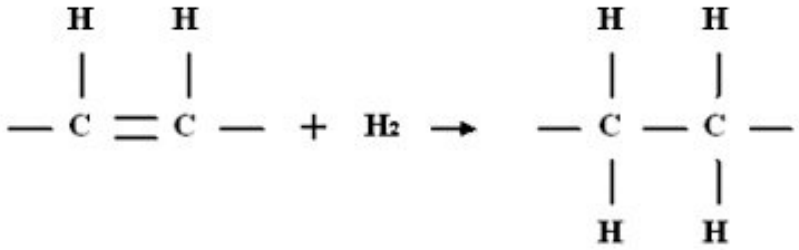

Figure 3.4 Hydrogenation of alkenes to alkanes

The hydrogenation of CO_2 into CH_4 describe simply as follow:

$$CO_2 + 4H_2 \longrightarrow CH_4 + 2H_2O \qquad (1)$$

This reaction is exothermic (ΔH = -170 kJ/mol of CO_2) and ΔG is -90 to -50 kJ/mol of CO_2 in the range between 473 and 773 K. Hydrogenation reactions are strongly exothermic so the reaction generally conducted in liquid phase to remove generated heat. If thermodynamic factors are consider, this reaction will not be limit. Hence, two reactions are following from first reaction. The following reactions are reverse water-gas shift and Fisher-Tropsch synthesis.

Reverse water-gas shift reaction (RWGS)[20]

Water-gas shift (WGS) reaction is primarily reaction to produce high-purity of H_2. WGS is exothermic reaction. If the reaction operates at low temperature, reverse water gas shift will happen. The Water-gas shift reaction as shown:

$$H_2O_{(g)} + CO_{(g)} \longrightarrow H_{2(g)} + CO_{2(g)}$$

Redox mechanisms for WGS are shown:

1. $H_2O(g) + * \rightleftarrows H_2O^*$;
2. $H_2O^* + * \rightarrow H^* + OH^*$ (RCS);
3. $2OH^* \rightleftarrows H_2O^* + O^*$;
4. $OH^* + * \rightarrow O^* + H^*$ (RCS);
5. $2H^* \rightleftarrows H_2(g) + 2^*$;
6. $CO(g) + * \rightleftarrows CO^*$;
7. $CO^* + O^* \rightarrow CO_2^* + *$ (RCS);
8. $CO_2^* \rightleftarrows CO_2(g) + *$;
9. $H^* + CO_2^* \rightleftarrows HCOO^* + *$.

* Symbol represents a surface site consisting of active metal atoms catalyst. Elementary reaction steps 2, 4 and 7 are rate-controlling steps.

Reverse water-gas shift reaction (RWGS) is the reaction between CO_2 and H_2 in metal catalyst. The products from RWGS are H_2O and CO.

There are two assumptions for RWGS mechanism.

- Redox reaction

Metal is oxidizer for CO_2 to be CO and Oxidizer is reduced by H_2 to be H_2O.

- Formate decomposition

CO is produces by decomposition of formate from CO2 and hydrogen in intermediate compound.

Reverse water-gas shift reaction as shown:

$$CO_{2(g)} + H_{2(g)} \longrightarrow CO_{(g)} + H_2O_{(g)} \qquad (2)$$

Fisher-Tropsch synthesis (FTS)[21]

Fischer-Tropsch is the reaction of syngas (mixture of CO and H_2) and products from reaction are hydrocarbon and H_2O. FTS is crucial technology to produce transportation fuels and chemicals. Commercial catalysts for FTS are Co and Fe. Products from difference catalysts in FTS are dissimilar. Co catalysts give long chain hydrocarbon which crack to gasoline or diesel fuel while high temperature process at 300-350°C on Fe catalyst use for production of $C5^+$ and operating temperature at 200-400°C give wax.

$$CO + 3H_2 \longrightarrow CH_4 + H_2O \qquad (3)$$

CHAPTER IV

EXPERIMENTAL

4.1 Research methodology

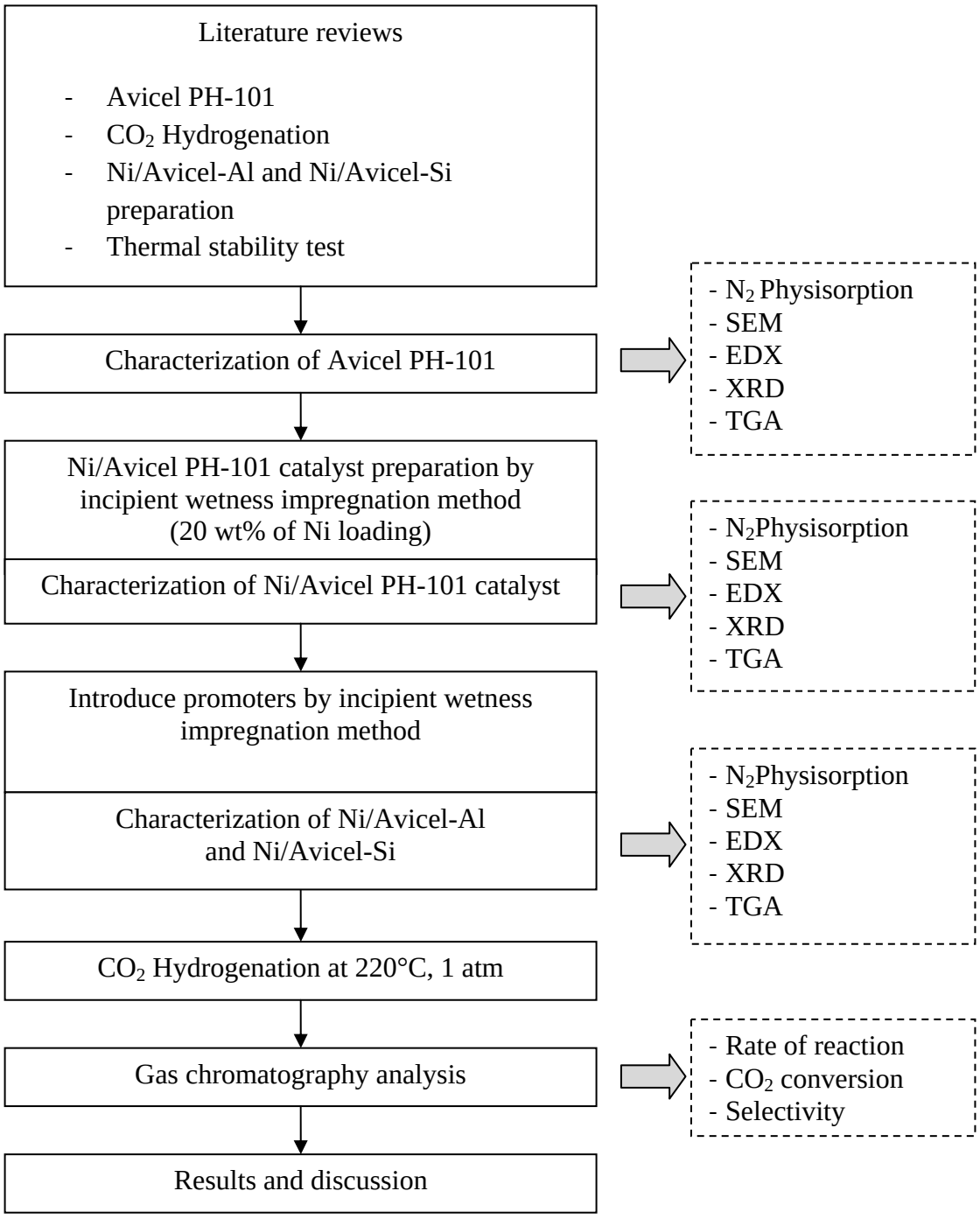

4.2 Catalyst preparation

Chemicals

- Avicel PH-101
- Nickel(II) nitrate hexahydrate [$Ni(NO_3)_2 \cdot 6H_2O$]
- Aluminium(III) nitrate [$Al(NO_3)_3$]
- Tetraethyl Orthosilicate [$Si(OC_2H_5)_4$]

Preparation Ni/Avicel PH101

- Dissolved 20 wt% loading of Nickel (II) nitrate hexahydrate [$Ni(NO_3)_2 \cdot 6H_2O$] in deionized water and impregnate to Avicel PH101.
- Dried catalyst precursor at 100°C for 12hr.
- Calcined in air at 200°C for 4 hr.

Preparation Ni/Avicel PH101-Al

- Dissolved 2, 6 and 12 wt% loading of aluminium(III) nitrate [$Al(NO_3)_3$] in deionized water and impregnate on Avicel PH101.
- Dried catalyst precursor at 100°C for 12hr.
- Calcined in nitrogen gas at 200°C for 4 hr.
- Dissolved 20 wt% loading of Nickel (II) nitrate hexahydrate [$Ni(NO_3)_2 \cdot 6H_2O$] in deionized water and impregnate to Avicel PH101.
- Dried catalyst precursor at 100°C for 12hr.
- Calcined in air at 200°C for 4 hr.

Preparation Ni/Avicel PH101-Si

- Dissolved 2, 6 and 12 wt% loading of tetraethyl orthosilicate [$Si(OC_2H_5)_4$] in deionized water and impregnate on Avicel PH101.
- Dried catalyst precursor at 100°C for 12hr.

- Calcined in nitrogen gas at 200°C for 4 hr.
- Dissolved 20 wt% loading of Nickel (II) nitrate hexahydrate [$Ni(NO_3)_2 \cdot 6H_2O$] in deionized water and impregnate to Avicel PH101
- Dried catalyst precursor at 100°C for 12hr.
- Calcined in air at 200°C for 4 hr.

4.3 Catalyst characterization

N_2 Physisorption (BET specific surface areas determination)

N_2 Physisorption (BET specific surface areas determination) is the method to determine surface area, pore size, pore volume and pore size distribution by micrometritic chemisorbs ASAP2620. The most common procedure for determining the internal surface area of a mesoporous material is based on adsorption and condensation of N_2 at liquid N_2 temperature (-196.15°C) using static vacuum procedures. Each adsorbed molecule occupies an area of cross-sectional area (0.162 nm^2). By measuring the number of N_2 molecules adsorbed at monolayer coverage, one can calculate the internal surface area.

SEM (Scanning electron microscope)

SEM (Scanning electron microscope) is widely used to identify morphology based on qualitative chemical analysis and/or crystalline structure by JSM-5800VL from JEOL. SEM is a type of electron microscope that images a sample by scanning with electron beam in a raster scan pattern. When electrons interact with the atoms the sample will produce signals that contain information about the sample's surface photography, composition, and other properties.

XRD (Phase analysis by X-ray diffraction)

XRD (Phase analysis by X-ray diffraction) is the technique to determine chemical composition of crystalline by repetitive arrangements of atoms which each

element has own unique diffraction pattern. The angle of diffraction by X-rays is measured by Siemens D5000 X-ray diffractometer with Cu K_α radiation with Ni filter.

Limitation of XRD as shown:

Range of 2θ: 10-80°

Resolution: 0.04°

Scanning circle: 10

TGA (Thermal gravimetric analysis)

TGA (Thermal gravimetric analysis) is a very convenient method for evaluate the oxidation state of component by reduction or oxidization sample in controlled environment and measure the weight variation by Perkin Elmer analysis diamond TG/DTA.

4.4 Apparatus

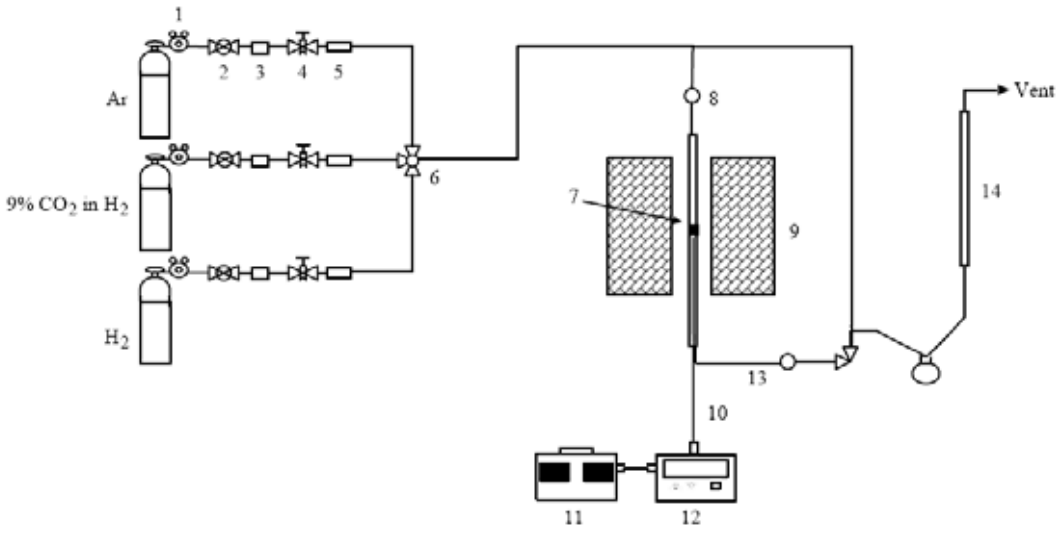

1. Pressure Regulator	2. On-Off Value	3. Gas Filter	4. Metering Valve
5. Back Pressure	6. 3-way Valve	7. Catalyst Bed	8. Sampling point
9. Furnace	10. Thermocouple	11. Variable Voltage Transformer	
12. Temperature Controller	13. Heating Line	14. Bubble Flow Meter	

Figure 4.1 Flow diagram of carbon dioxide hydrogenation system

Reactor

Fixed bed reactor was made from stainless steel tube, 3/8”outside diameter. The catalyst was packed between quartz wood layers in reactor.

Automatic temperature controller

Magnetic switch, transformer and temperature controller (model no. SS2425DZ) was connected to temperature transmitter to show the variation of temperature. The suitable temperature is 0-800°C at 220VAC

Electrical furnace

The heating in carbon dioxide hydrogenation reactor was produced from electrical furnace. Maximum temperature from electrical furnace is 800°C at 220VAC

Gas controlling system

Gas flow rate was controlled by pressure regulator, on-off valve and metering valve.

Gas chromatography

CO_2 and CO from feed and product were analyzed by Shimadzu GC8A (thermal conductive detector gas chromatography, molecular sieve 5A). Shimazu GC14B (VZ10), frame ionization detector gas chromatography, was used to analyze hydrocarbon composition from reaction. Gas chromatography specifications are shown:

Table 4.1 Gas chromatography specifications

Gas Chromagraph	SHIMADZU GC-8A	SHIMADZU GC-14B
Detector	TCD	FID
Column	Molecular sieve 5Å	VZ10
- Column material	SUS	-
- Length	2 m	-
- Outer diameter	4 mm	-
- Inner diameter	3 mm	-
- Mesh range	60/80	60/80
-Maximum temperature	350 ^{o}C	80^{o}C
Carrier gas	He (99.999%)	H_2 (99.999%)
Carrier gas flow	40 cc/min	-
Column gas	He (99.999%)	Air, H_2
Column gas flow	40 cc/min	-

Gas Chromagraph	SHIMADZU GC-8A	SHIMADZU GC-14B
Column temperature		
- initial (^oC)	60	70
- final (^oC)	60	70
Injector temperature (^oC)	100	100
Detector temperature (^oC)	100	150
Current (mA)	80	-
Analysed gas	Ar, CO, CO_2, H_2	Hydrocarbon C_1-C_4

Reaction test

Sample (0.1 g) was packed in a fixed-bed microreactor. Sample was reduced by H_2 (50ml/min) at 220°C for 5 hr. to change nickel oxide to metal. Ar (8ml/min) and H_2 (22ml/min) was flowed to reduce CO_2 before start reaction and record concentration of CO_2 in feed by gas chromatography. CO_2 hydrogenation was carried out at 220°C and 1 atm. Steady state was reached in 5 hr. The sample from reactor was analyzed every 1 hr by gas chromatography to determine CO_2, CO and CH_4 composition.

- % CO_2 conversion calculation

$$\%\ CO_2 \text{ conversion} = \frac{100 \times [mole of\ CO_2\ in\ feed - mole of\ CO_2\ in\ product]}{mole of\ CO_2\ in\ feed}$$

- Reaction rate (g CH_2/gcat·h)

$$\text{Reaction rate} = \frac{\%\ CO_2 \text{ conversion} \times \text{feed flow rate of } CO_2\ (\text{cm}^3/\text{min}) - \text{ mole of } CH_2\ (\text{g/mol})}{\text{catalyst weight (g)} \times 22{,}400\ (\text{cm}^3/\text{mol})}$$

CHAPTER V

RESULT AND DISCUSSION

This chapter was separated into 3 parts. The first part contains the characterization and catalyst activity of avicel supported nickel catalysts. The second part displays characterization and catalytic activity of aluminium modification of cellulose supported nickel catalysts. The last part presents characterization and catalytic activity of silicon modification of avicel supported nickel catalysts. The catalytic properties of all parts were studied over carbon dioxide hydrogenation reaction under methanation condition at 200°C, 1 atm for 5 hr.

5.1 Characterization and catalyst activity of avicel supported nickel catalyst

5.1.1 Characterization of avicel and avicel supported nickel catalysts

5.1.1.1 Scanning electron microscope (SEM)

The surface structures of support and cellulose supported nickel catalysts were characterized by scanning electron microscope (SEM). Figure 5.1(a) and Figure 5.1(b) show SEM images of cellulose at scale 10 and 50 μm, respectively. The surface of cellulose showed roughness shape and layer of amorphous structure.

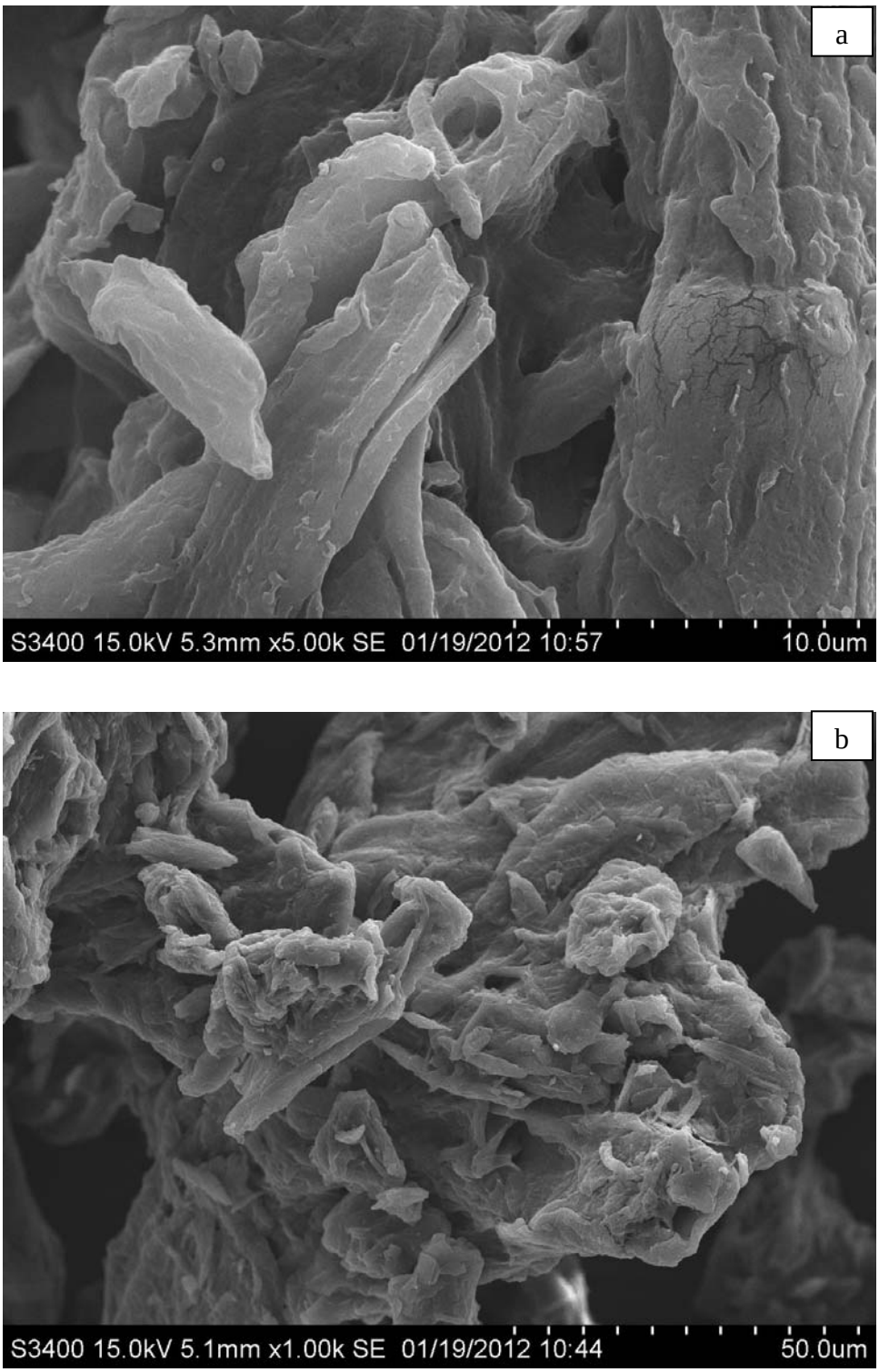

Figure 5.1 SEM micrographs of support, Avicel: (a) Avicel (scale 10 μm), (b) Avicel (scale 50 μm)

Ni (20% wt) was impregnated on Avicel PH101 and dried at 100°C for 24 hr. Then, the samples were calcined under air condition at 200°C for 4 hr. The surfaces of cellulose were covered with a large amount of nickel particle (white patches) on sample surface as shown in Figure 5.2(a) and Figure 5.2(b).

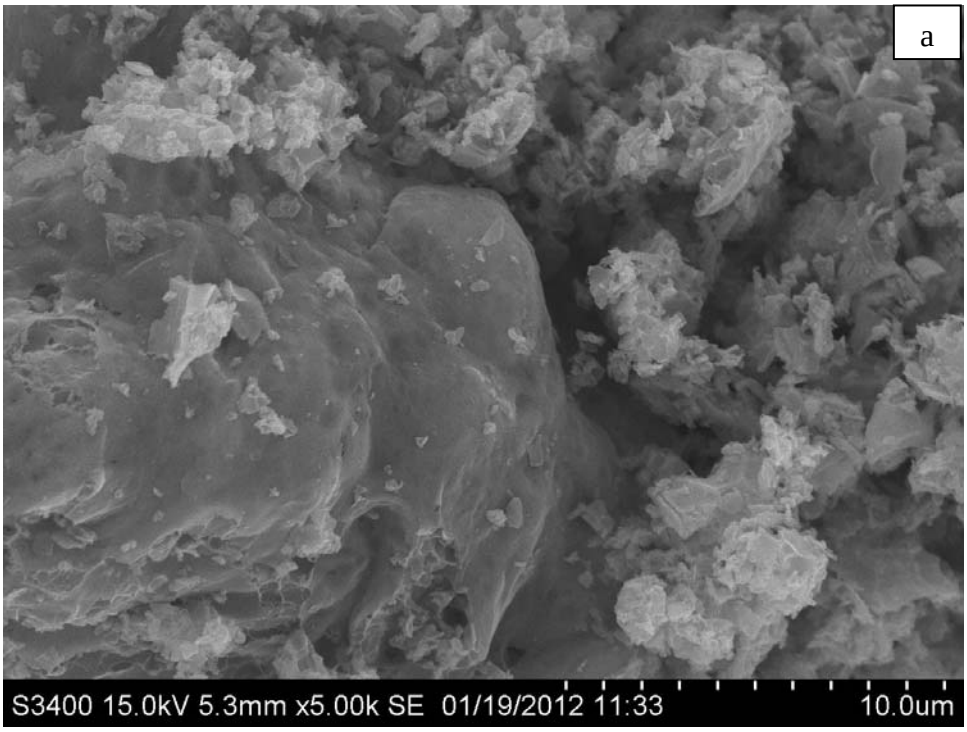

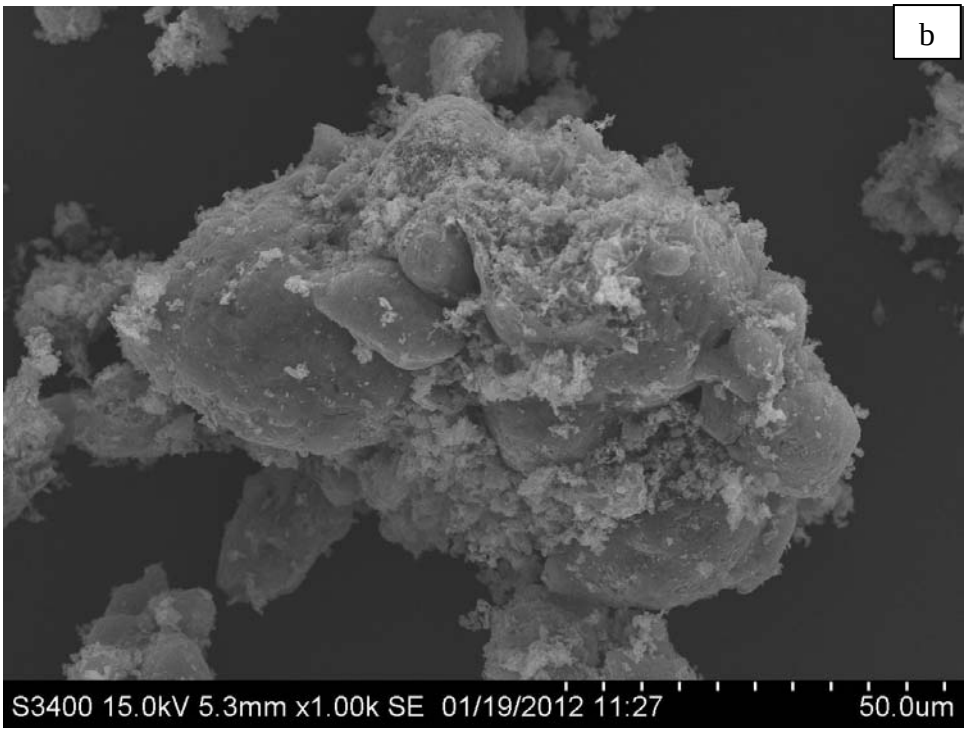

Figure 5.2 SEM micrographs of avicel supported nickel (20 wt%) catalyst, Ni/AV: (a) 20 wt% Ni/AV (scale 10 μm), (b) 20 wt% Ni/AV (scale 50 μm)

5.1.1.2 Eergy dispersive X-ray spectroscopy (EDX)

Composition and distribution of samples were determined by energy dispersive X-ray spectroscopy (EDX). EDX mapping illustrates the distribution of species in the near-surface region or 1-5μm depth from surface. EDX mapping images of AV were displayed in Fig 5.3. The results in table 5.1 showed that AV composes of carbon 56.25 wt% and oxygen 43.75 wt%, respectively.

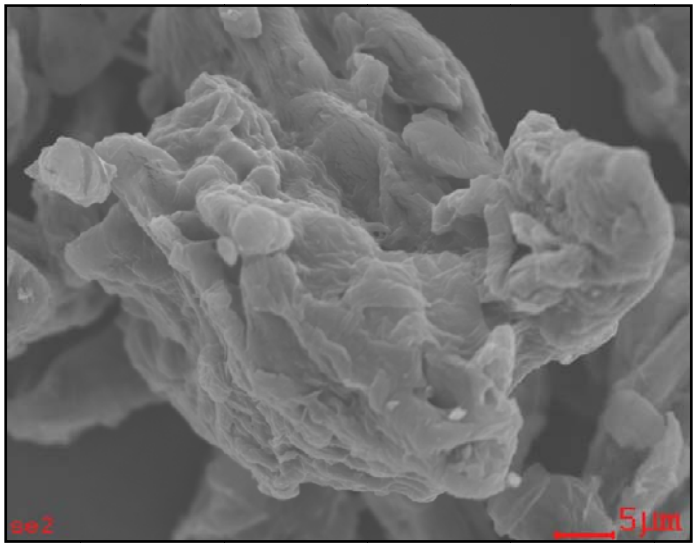

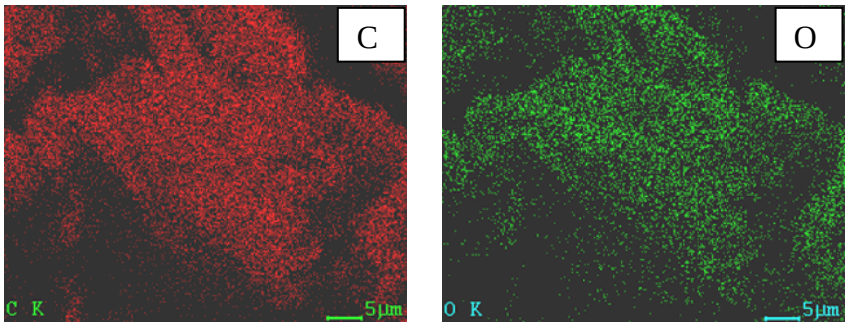

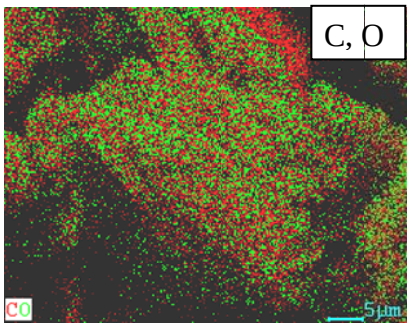

Figure 5.3 EDX mapping images of cellulose

Table 5.1 Determine composition of cellulose by energy dispersive X-ray spectroscopy (EDX)

Samples	wt%		at%	
	C	O	C	O
AV	56.25	43.75	63.14	36.86

Figure 5.4, the images perform EDX mapping of cellulose supported nickel (20%wt) catalysts. The catalysts were well-dispersed with nickel atom, which can be clearly seen in Figure 5.4. Table 5.2 shows the composition of samples in weight percentage and atoms percentage. Nickel particles were found in samples at 32.21 wt% or 9.31 at%.

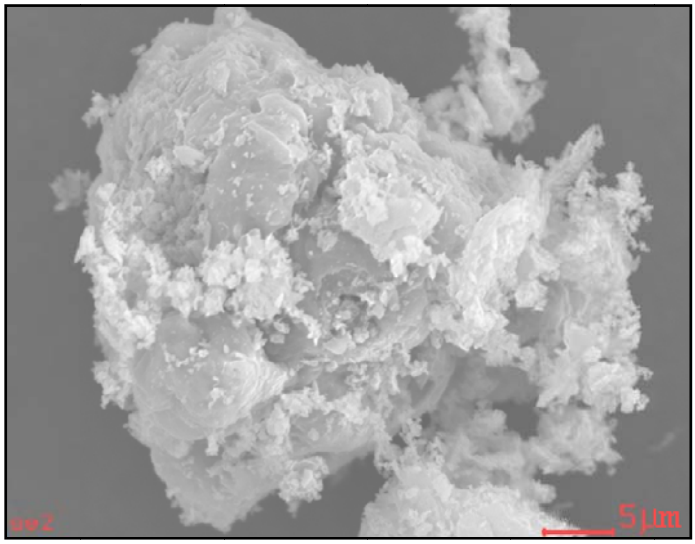

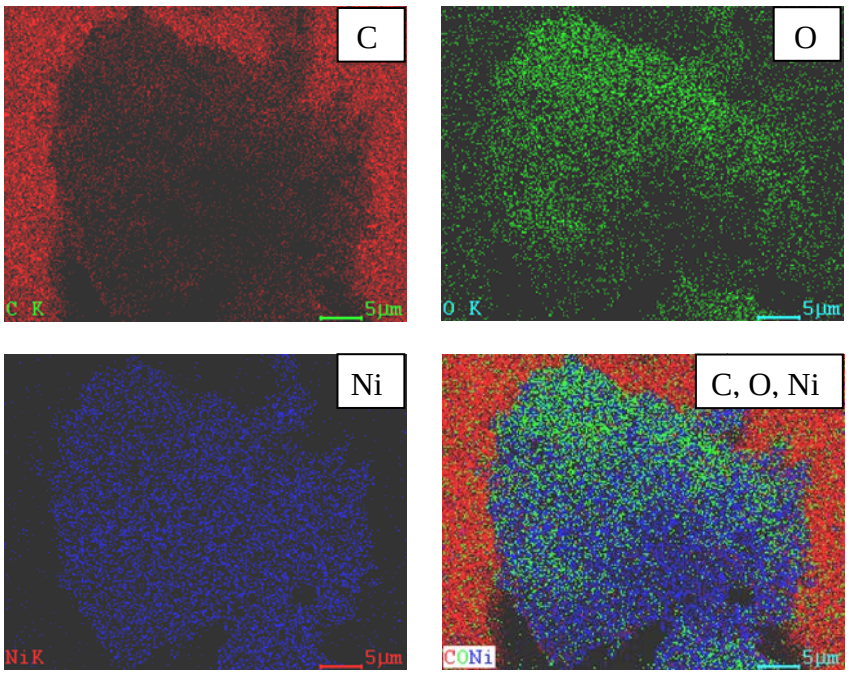

Figure 5.4 EDX mapping images of avicel supported nickel

Table 5.2 Determine composition of avicel supported nickel by energy dispersive

X-ray spectroscopy (EDX)

Samples	wt%			at%		
	C	O	Ni	C	O	Ni
Ni/AV	53.46	14.33	32.21	75.50	15.20	9.31

5.1.1.3 Phase analysis by X-ray diffraction (XRD)

XRD (Phase analysis by X-ray diffraction) was used to characterize the chemical composition of crystalline by repetitive arrangements of atoms which each element has own unique diffraction pattern. XRD methods for crystallite size determination are applicable to crystallites in the range of 2-100 nm. The diffraction peaks are very broad for crystallites below 2-3 nm, while for particles with size above 100 nm the peak broadening is too small. The samples were analyzed at diffraction angles between 20° to 80°. XRD patterns of supports and nickel loading of 20 % by

weight supported avicel catalysts followed by calcined under air condition at 200°C, 1 atm for 4 hr are shown in Figure 5.5. The XRD images of AV show peaks at 2θ of 15, 22.5 and 35. From XRD images of nickel loading of 20 % by weight supported avicel catalysts, the graph demonstrates XRD peaks at 2θ of 13, 38, 45, 53 and 63. XRD peaks at 2θ of 38 and 63 exhibited nickel oxide (NiO) and 2θ of 45 and 53 displayed nickel. [22-26]

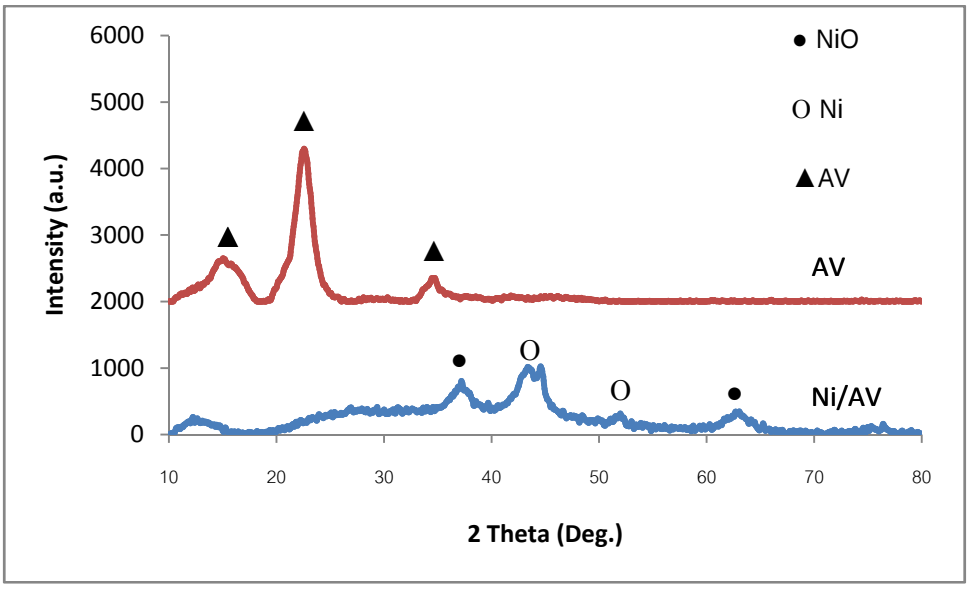

Figure 5.5 XRD patterns of avicel and avicel supported nickel

5.1.1.4 N_2 Physisorption (BET specific surface areas determination)

Surface area of support and cellulose supported nickel was determined by N_2 physisorption (BET). The results showed surface area of support and cellulose supported nickel was 7.6 and 48.9 m^2/g, respectively. The surface area of cellulose supported nickel was higher than cellulose because layer of nickel and nickel oxide covered on cellulose.

5.1.1.5 TGA (Thermal gravimetric analysis)

TGA (Thermal gravimetric analysis) is a very convenient method for evaluate the oxidation state of component by reduce or oxidize sample in controlled environment and measure the weight variation. The samples were examined at

temperature between 30-200°C. Figure 5.6 displays TGA profile of support and avilcel supported nickel after calcinations. Weight loss of avicel and avicel supported nickel are shown 8.7 and 3.5 wt%, respectively. From TGA profile of cellulose or avicel, moisture in sample was initially removed from 25°C to 100°C and organics parts were decomposed after 100°C. For TGA profile of cellulose supported nickel, moisture in sample was initially removed from 25°C to 100°C. After 100°C organics parts were decomposed and nickel oxide was transformed to nickel.

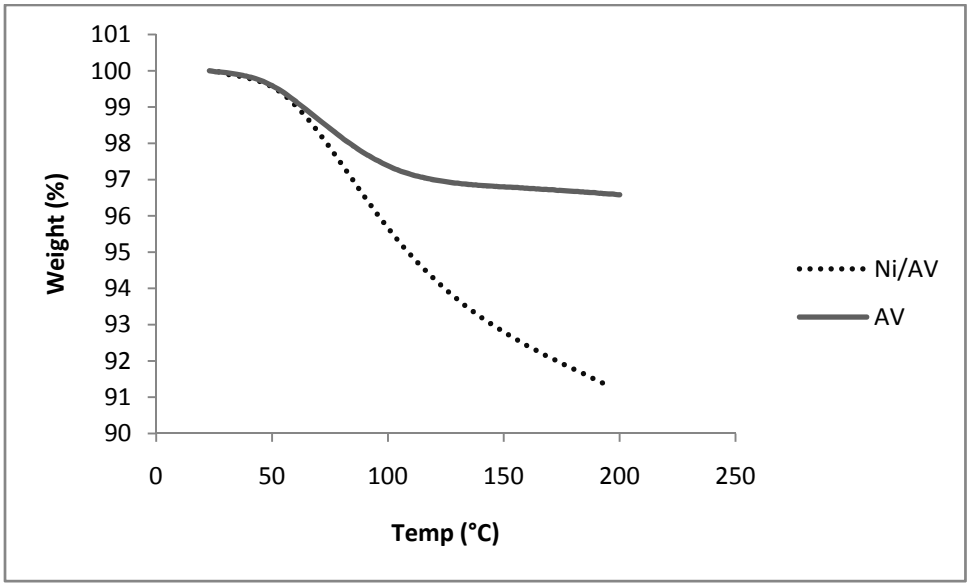

Figure 5.6 TGA analysis characterizing weight loss (%) of avicel and avicel supported nickel

5.1.2 Catalyst activity

CO_2 hydrogenation was carried out in fixed bed reactor. The main product and by products in this experiment were methane and carbon dioxide, respectively. Sample (0.1 g) was packed in a fixed-bed microreactor. Sample was reduced by H_2 (50ml/min) at 220°C for 5 hr. to change nickel oxide to metal. Ar (8ml/min) and H_2 (22ml/min) was flew to reduce CO_2 before start reaction and record concentration of CO_2 in feed by gas chromatography. CO_2 hydrogenation was carried out at 220°C and 1 atm. Steady state was reached in 5 hr. The sample from reactor was analyzed every

1 hr by gas chromatography to determine CO_2, CO and CH_4 composition. CO_2 conversion (%), selectivity (%) and rate of reaction are shown in table 5.3.

Table 5.3 Catalyst activity of avicel supported nickel

Catalysts	CO_2 conversion (%)	Selectivity (%)		Rate of reaction
	Steady state	CH_4	CO	(gCH_2/gcat.hr)
Ni/AV	23.20	87.88	12.12	14.92

5.2 Characterization and catalytic activity of aluminium modification of cellulose supported nickel catalysts

5.2.1 Characterization of aluminium modification of cellulose supported nickel catalysts

5.2.1.1 Scanning electron microscope (SEM)

Ni (20 %wt) was impregnated onto the aluminium modification (2, 6 and 12 %wt) of Avicel PH101 and dried at 100°C for 24 hr. Then, the samples were calcined under air condition at 200°C for 24 hr. The surfaces of samples were covered with a large amount of nickel particle and alumina as shown in Figure 5.7 to Figure 5.9.

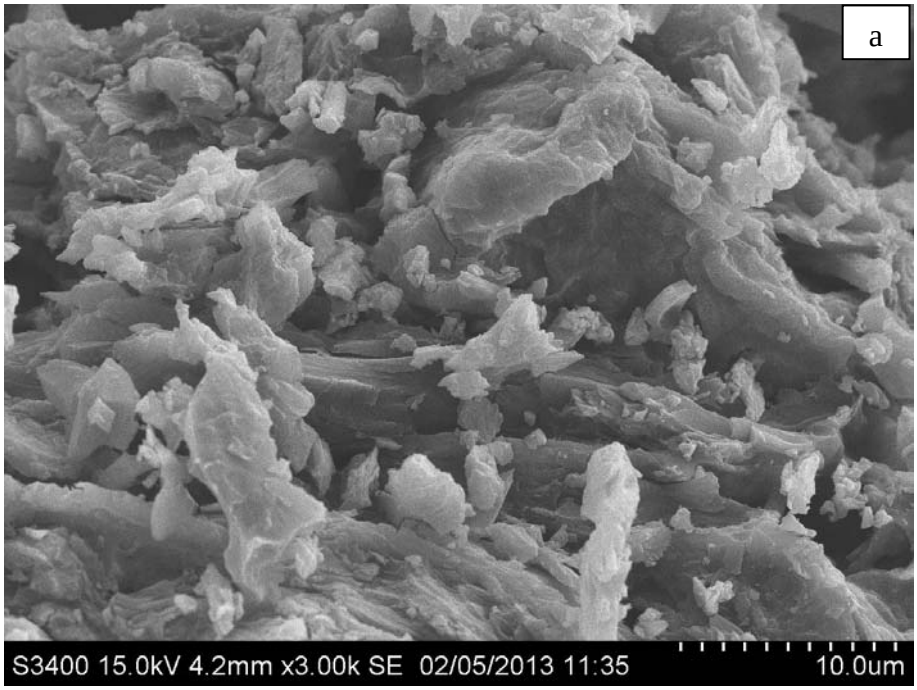

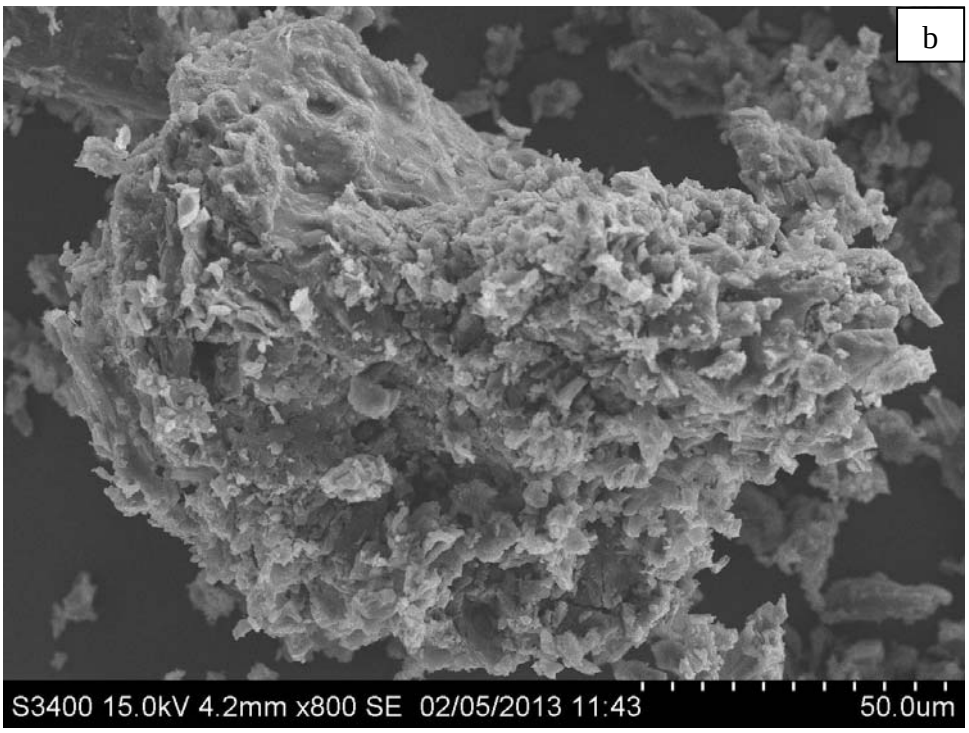

Figure 5.7 SEM micrographs of aluminium (2 wt%) modification avicel supported nickel (20 wt%) catalyst, Ni/AV: (a) 20 wt% Ni/AV-2Al (scale 10 μm), (b) 20 wt% Ni/AV-2Al (scale 50 μm)

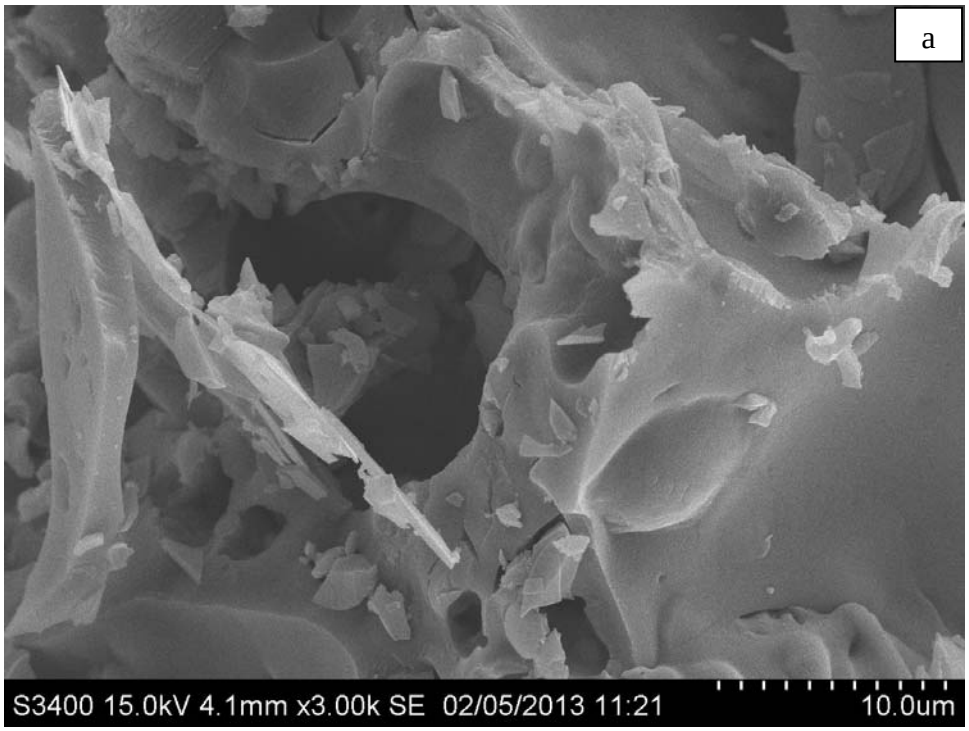

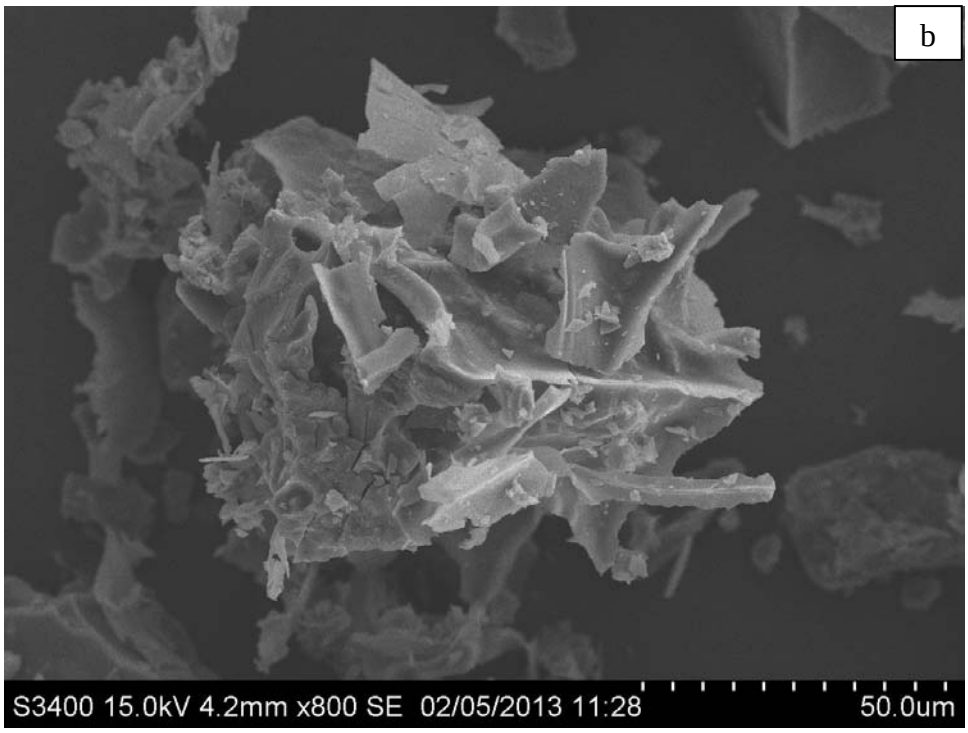

Figure 5.8 SEM micrographs of aluminium (6 wt%) modification avicel supported nickel (20 wt%) catalyst, Ni/AV: (a) 20 wt% Ni/AV-6Al (scale 10 μm), (b) 20 wt% Ni/AV-6Al (scale 50 μm)

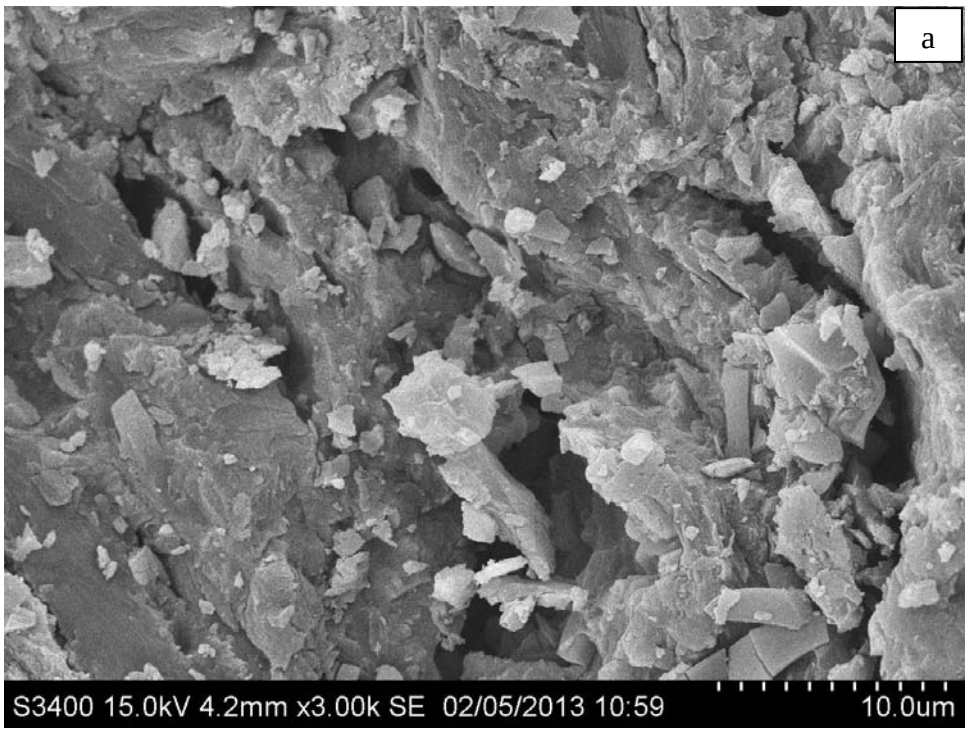

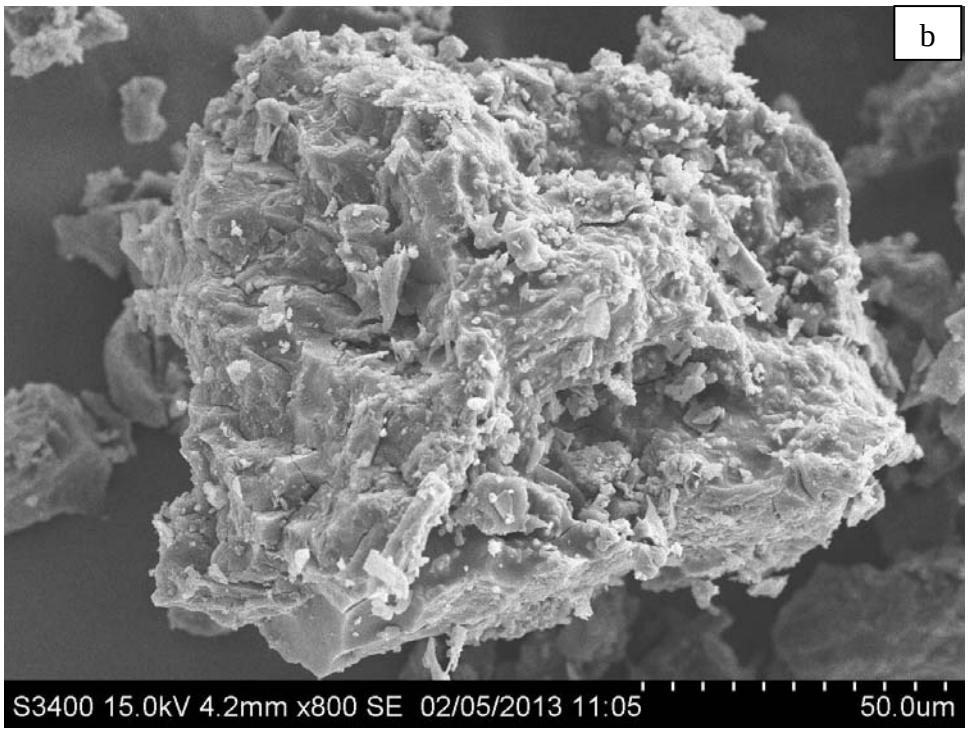

Figure 5.9 SEM micrographs of aluminium (12 wt%) modification avicel supported nickel (20 wt%) catalyst, Ni/AV: (a) 20 wt% Ni/AV-12Al (scale 10 μm), (b) 20 wt% Ni/AV-12Al (scale 50 μm)

5.2.1.2 Energy dispersive X-ray spectroscopy (EDX)

Composition and dispersion of samples were determined by energy dispersive X-ray spectroscopy (EDX). EDS mapping illustrates the distribution of species in the near-surface region or 1-5μm depth from surface. Ni (20 %wt) was impregnated onto aluminium modification (2, 6 and 12 %wt) of Avicel PH101 and dried at 100°C for 24 hr. Then, the samples were calcined under air condition at 200°C for 24 hr. Catalysts were well-dispersed with nickel atom and aluminium atom, which can be clearly seen in Figure 5.10 to Figure 5.12.

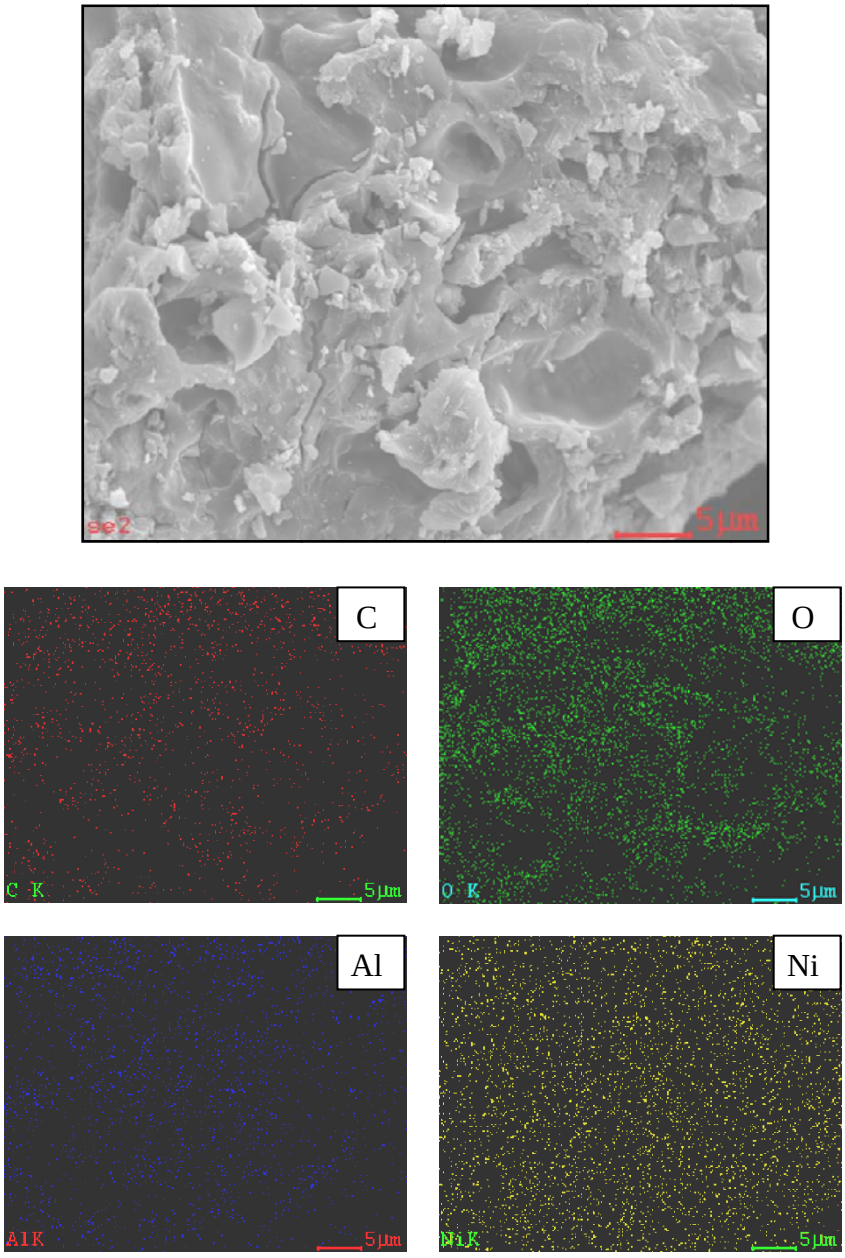

Figure 5.10 EDX mapping images of aluminium (2 wt%) modification avicel supported nickel (20 wt%) catalyst

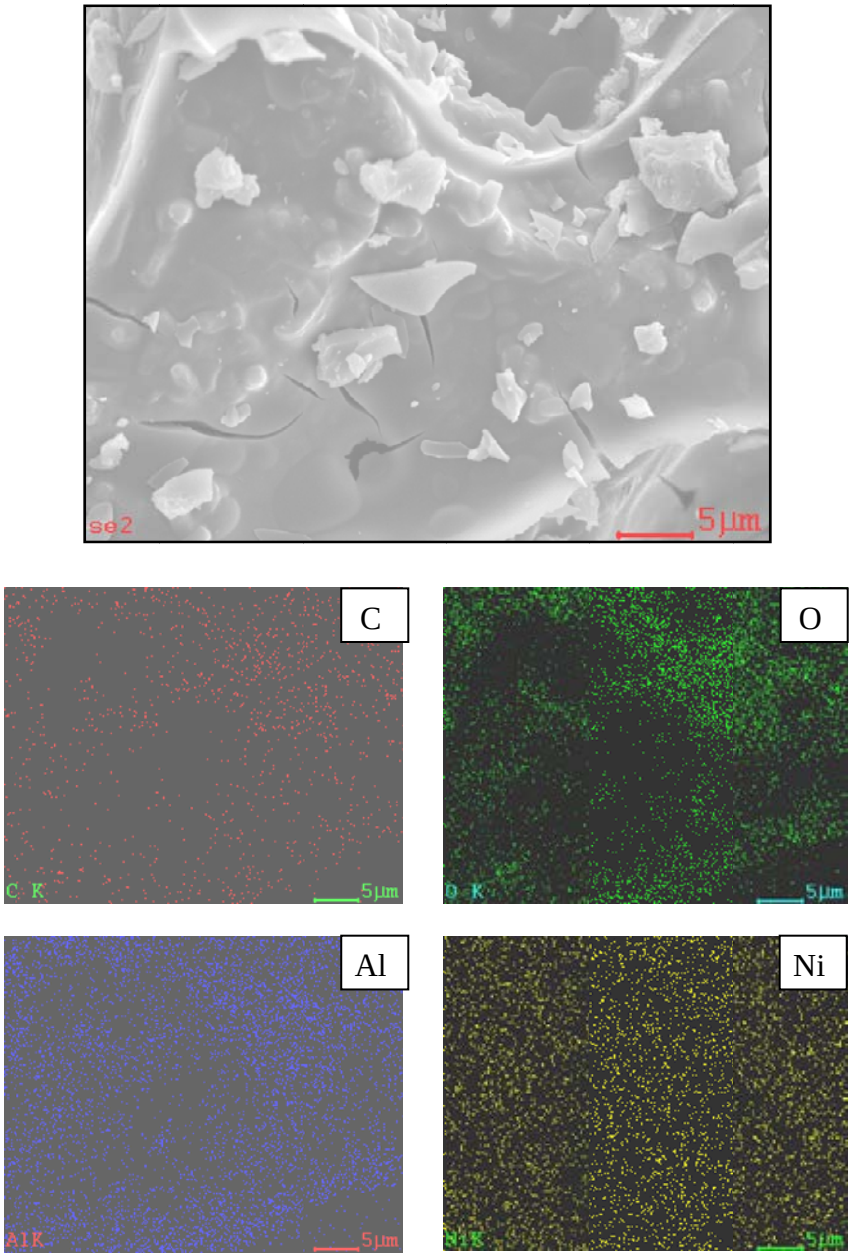

Figure 5.11 EDX mapping images of aluminium (6 wt%) modification avicel supported nickel (20 wt%) catalyst

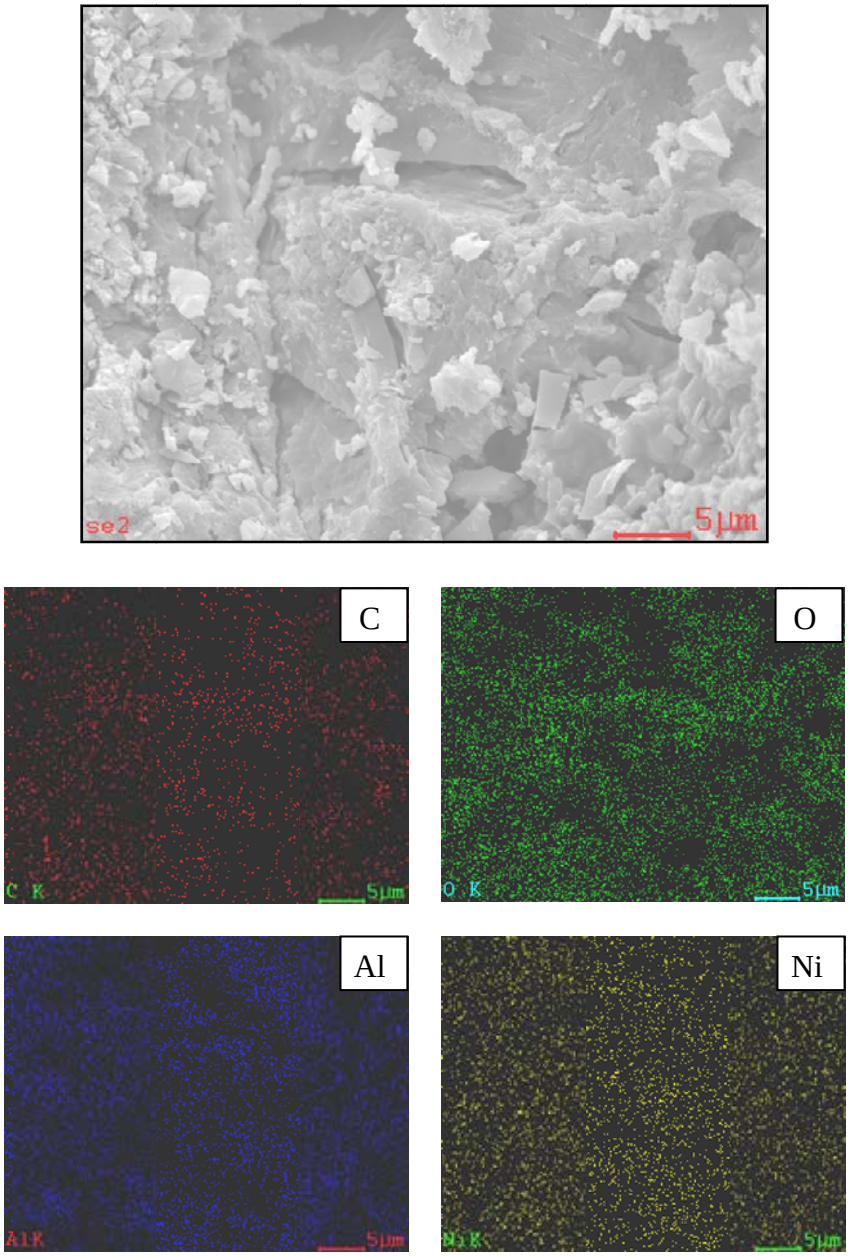

Figure 5.12 EDX mapping images of aluminium (12 wt%) modification avicel supported nickel (20 wt%) catalys

The compositions of samples are shown in weight percentage and atoms percentage, as seen in table 5.4. The results were displayed that the composition of samples were consisted of carbon, oxygen, aluminium and nickel. The highest nickel on surface or 1-5µm depth was obtained 56.63 wt% and 26.98 at% at 6 wt% of alumina.

Table 5.4 Determine composition of avicel supported nickel by energy dispersive X-ray spectroscopy (EDX)

Samples	wt%				at%			
	C	O	Al	Ni	C	O	Al	Ni
Ni/AV-2Al	17.19	24.19	3.46	55.16	35.69	37.69	3.20	23.42
Ni/AV-6Al	9.13	22.52	11.82	56.53	21.31	39.44	12.27	26.98
Ni/AV-12Al	12.41	28.05	13.33	46.21	25.40	43.11	12.14	19.35

5.2.1.3 Phase analysis by X-ray diffraction (XRD)

XRD (Phase analysis by X-ray diffraction) was used to characterize the chemical composition of crystalline by repetitive arrangements of atoms which each element has own unique diffraction pattern. XRD methods for crystallite size determination are applicable to crystallites in the range of 2-100 nm. The diffraction peaks are very broad for crystallites below 2-3 nm, while for particles with size above 100 nm the peak broadening is too small. The samples were analyzed at diffraction angles between 20° to 80°. XRD patterns of various alumina modification avicel supported nickel followed by calcined under air condition at 200°C, 1 atm for 4 hr are shown in Figure 5.13. From XRD images of alumina modification supported nickel loading of 20 % by weight, all samples exhibited strong peaks at 2θ of 22.3° for avicel. For Ni/AV-6Al and Ni/AV-12Al, the slightly diffraction peaks of Ni can be observed at 2θ of 44°. Only the small diffraction peak of Ni/AV-12Al at 2θ of 43.4° can be displayed Ni. The diffraction peaks of all samples at 2θ of 19 and 35.8° belong to γ-Al_2O_3. The results indicated that γ-Al_2O_3 was highly dispersion in Ni/AV-6Al and Ni/AV-12Al. [22-26]

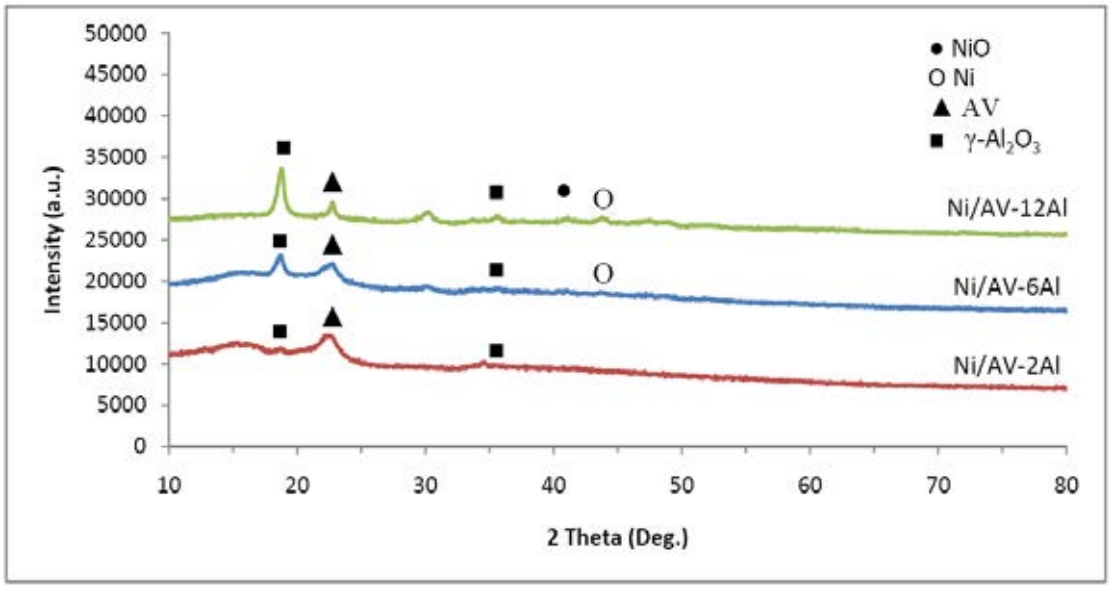

Figure 5.13 XRD patterns of alumina modification supported nickel catalysts by various alumina loading

5.2.1.4 N_2 Physisorption (BET sic surface areas determination)

Surface area of aluminium modification of cellulose supported nickel was determined by N_2 physisorption (BET). The results showed that surface area of Ni/AV-2Al, Ni/AV-6Al were 0.2065 and 0.0907 m^2/g, respectively. From the experiment, surface area was decreased when increase aluminium loading to the samples.

5.2.1.5 TGA (Thermal gravimetric analysis)

TGA (Thermal gravimetric analysis) is a very convenient method for evaluate the oxidation state of component by reduce or oxidize sample in controlled environment and measure the weight variation. The samples were examined at temperature between 30-200°C. Figure 5.14 shows TGA profile of various alumina modification avicel supported nickel followed by calcined under air condition at 200°C, 1 atm for 4 hr. From Figure 5.14, weight loss of Ni/AV-2Al and Ni/AV-12Al can be observed to 9%. Weight loss of Ni/AV-6Al was shown in the lowest line, 10% weight loss. Thus, thermal stability of Ni/AV-2Al and Ni/AV-12Al was satisfied

more than Ni/AV-6Al. From TGA profile of various alumina modification avicel supported nickel, moisture in sample was initially removed from 25°C to 100°C and organics parts were decomposed after 100°C. After 100°C, organics parts were decomposed and nickel oxide was transform to nickel.

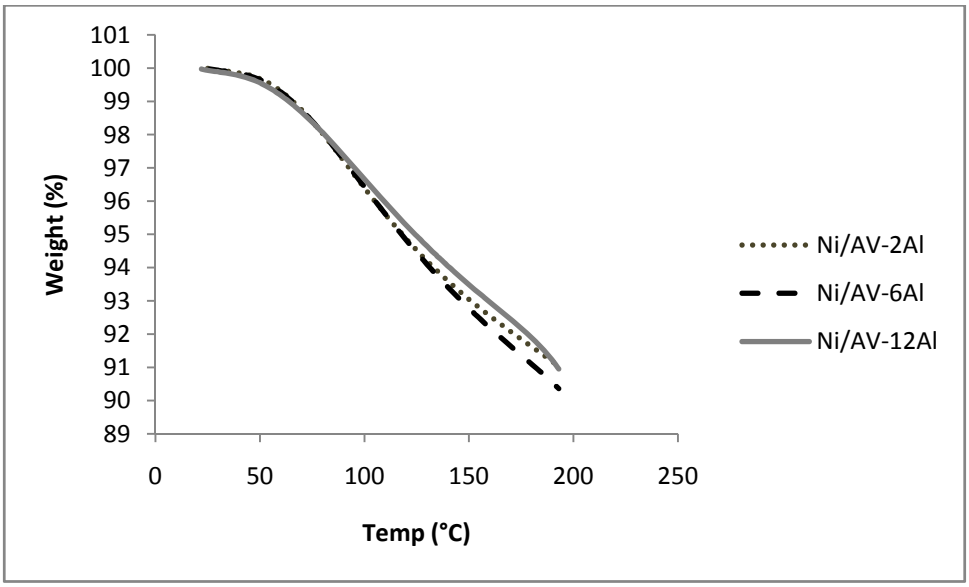

Figure 5.14 TGA analysis characterizing weight loss (%) of alumina modification supported nickel

5.2.2 Catalyst activity

CO_2 hydrogenation was carried out in fixed bed reactor. The main product and by products in this experiment were methane and carbon dioxide, respectively. Sample (0.1 g) was packed in a fixed-bed microreactor. Sample was reduced by H_2 (50ml/min) at 220°C for 5 hr. to change nickel oxide to metal. Ar (8ml/min) and H_2 (22ml/min) was flew to reduce CO_2 before start reaction and record concentration of CO_2 in feed by gas chromatography. CO_2 hydrogenation was carried out at 220°C and 1 atm. Steady state was reached in 5 hr. The sample from reactor was analyzed every 1 hr by gas chromatography to determine CO_2, CO and CH_4 composition. CO_2 conversions of alumina modification supported nickel at steady state were estimated to 72.41-99.51% and Ni/AV-6Al showed the highest CO_2 conversion. The selectivity to CH_4 was 25.19-39.87% and rate of reaction was 46.55-63.98 gCH_2/gcat.hr. By

changing alumina loading, the highest selectivity to CH_4 was obtained at 12 wt% of alumina. The optimum alumina loading to reach the highest rate of reaction was 6 wt%. CO_2 conversion (%), selectivity (%) and rate of reaction were shown in table 5.5.

Table 5.5 Catalyst activity of alumina modification supported nickel

Catalysts	CO_2 conversion (%)	Selectivity (%)		Rate of reaction
	Steady state	CH_4	CO	(gCH_2/gcat.hr)
Ni/AV-2Al	72.41	31.98	68.02	46.55
Ni/AV-6Al	161.75	25.34	74.66	103.99
Ni/AV-12Al	95.35	39.87	60.13	61.30

5.3 Characterization and catalytic activity of silicon modification of avicel supported nickel catalysts

5.3.1 Characterization of silicon modification of cellulose supported nickel catalysts

5.3.1.1 Scanning electron microscope (SEM)

Ni (20 %wt) was impregnated on silicon modification (2,6 and 12 %wt) Avicel PH101 and dried at 100°C for 24 hr. Then, the samples were calcined under air condition at 200°C for 24 hr. The surfaces of samples were covered with a large amount of nickel particle and silicon as shown in Figure 5.15 to Figure 5.17.

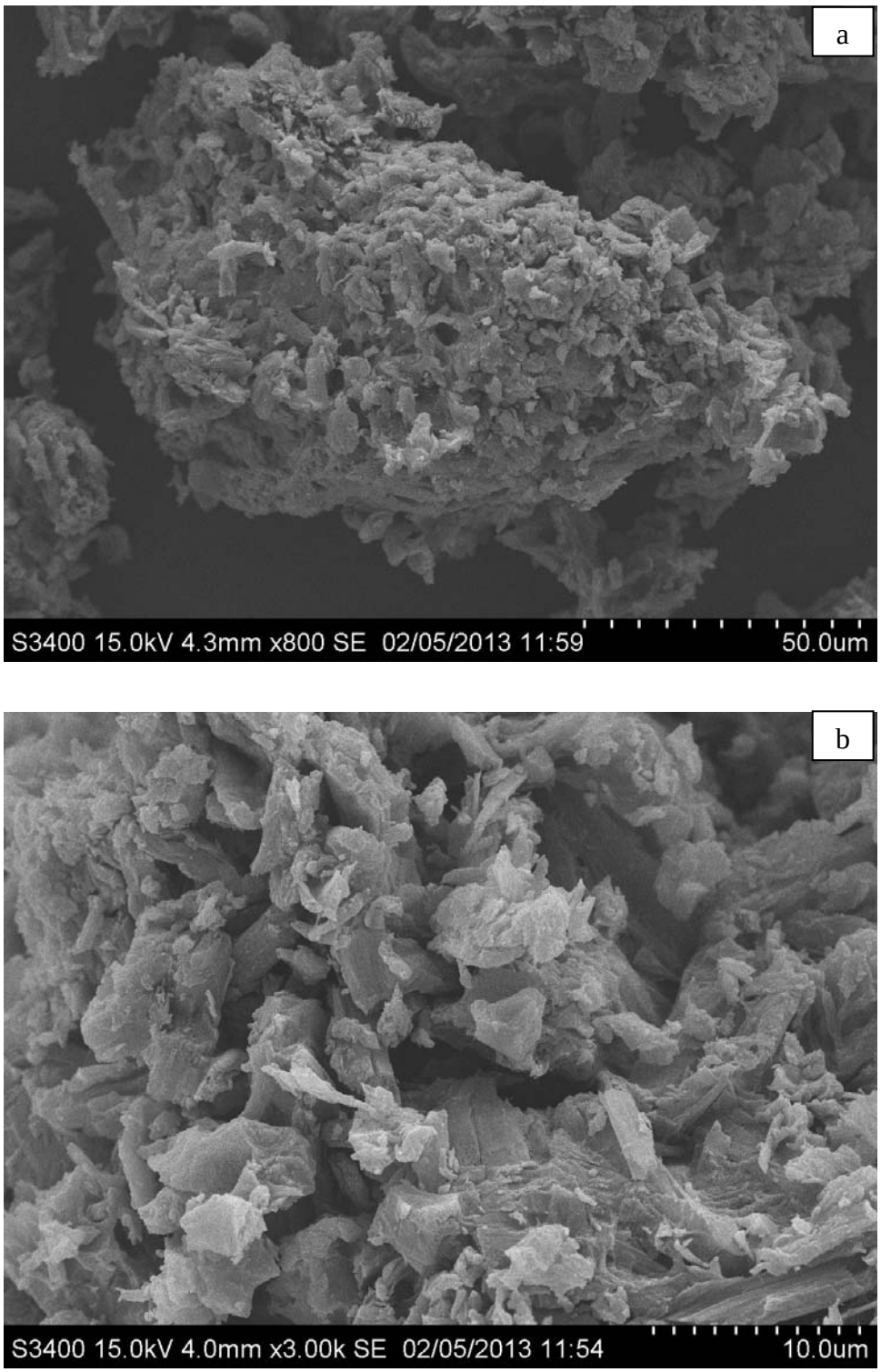

Figure 5.15 SEM micrographs of silicon (2 wt%) modification avicel supported nickel (20 wt%) catalyst, Ni/AV: (a) 20 wt% Ni/AV-2Si (scale 10 μm), (b) 20 wt% Ni/AV-2Si (scale 50 μm)

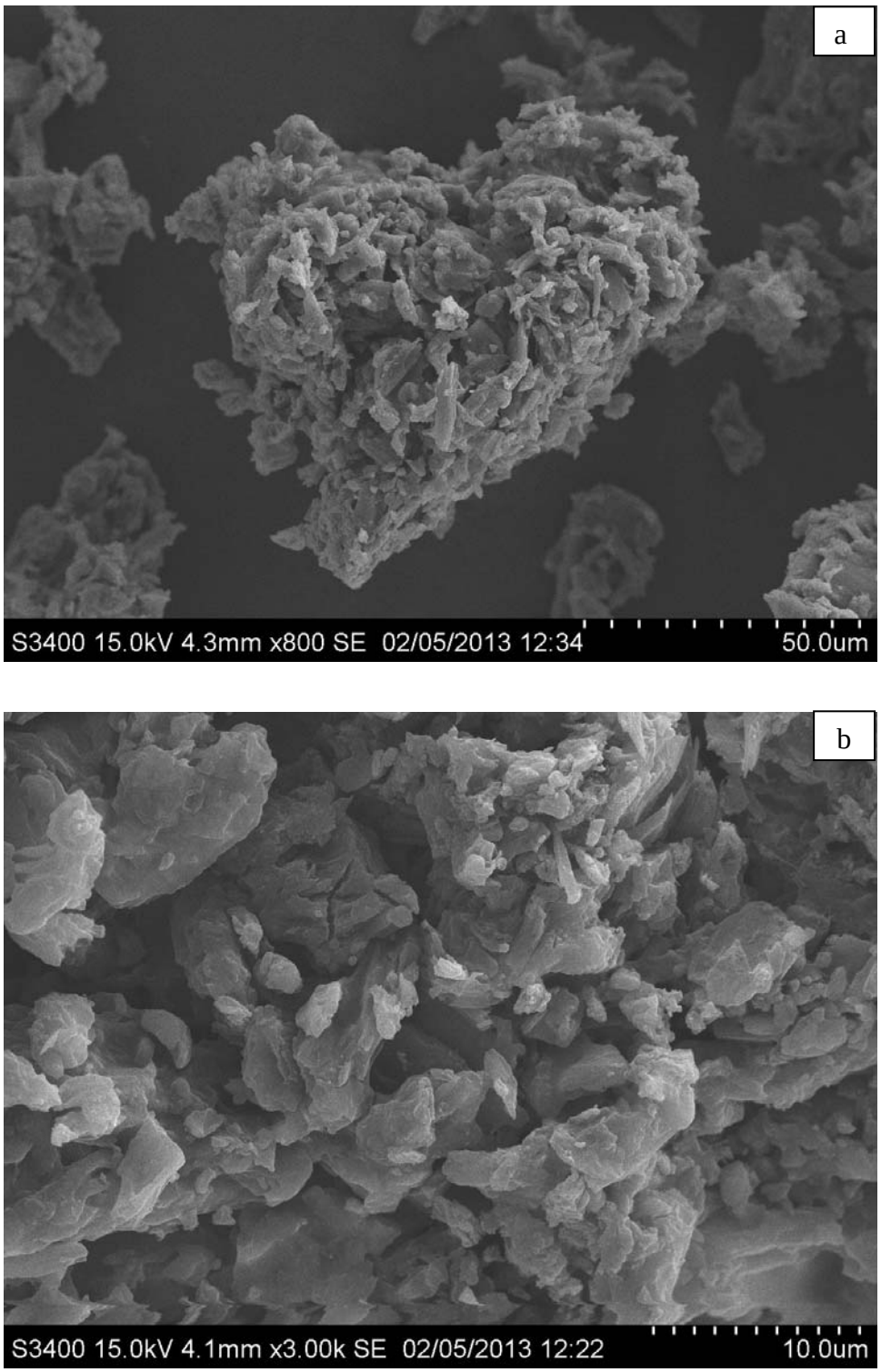

Figure 5.16 SEM micrographs of silicon (6 wt%) modification avicel supported nickel (20 wt%) catalyst, Ni/AV: (a) 20 wt% Ni/AV-6Si (scale 10 μm), (b) 20 wt% Ni/AV-6Si (scale 50 μm)

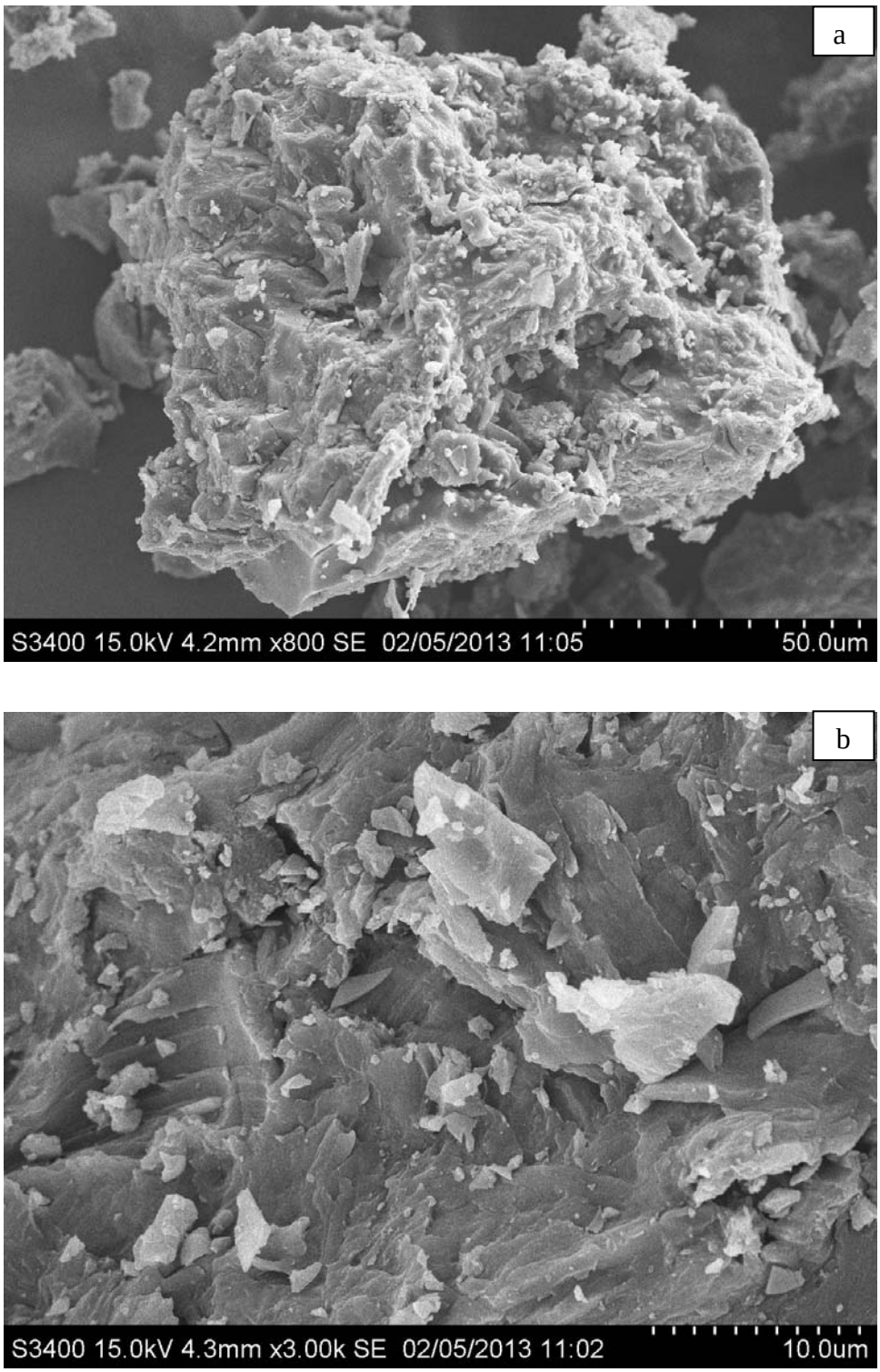

Figure 5.17 SEM micrographs of silicon (12 wt%) modification avicel supported nickel (20 wt%) catalyst, Ni/AV: (a) 20 wt% Ni/AV-12Si (scale 10 μm), (b) 20 wt% Ni/AV-12Si (scale 50 μm)

5.3.1.2 Eergy dispersive X-ray spectroscopy (EDX)

Composition and dispersion of samples were determined by energy dispersive X-ray spectroscopy (EDX). EDS mapping illustrates the distribution of species in the near-surface region or 1-5μm depth from surface. Ni (20 %wt) was impregnated on silicon modification (2,6 and 12 %wt) Avicel PH101 and dried at 100°C for 24 hr. Then, the samples were calcined under air condition at 200°C for 24 hr. Catalysts were well-dispersed with nickel atom and silicon atom, which can be clearly seen in Figure 5.18 to Figure 5.20.

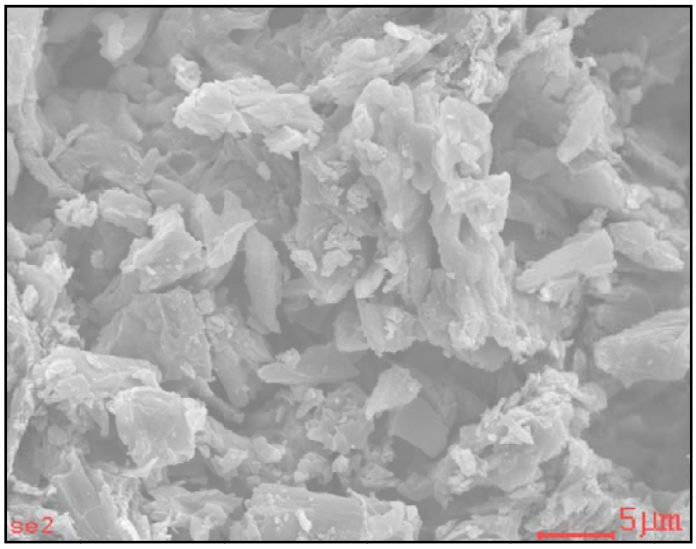

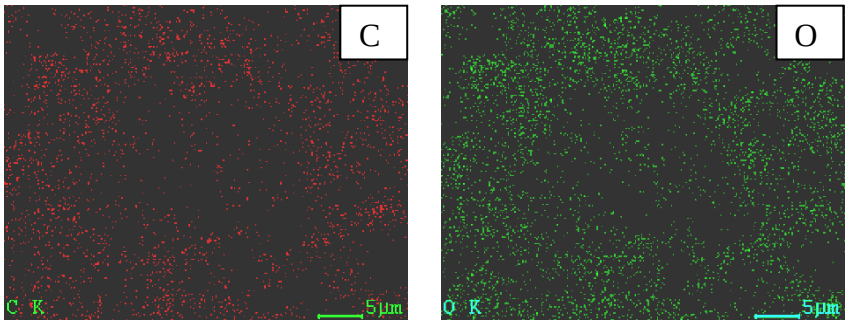

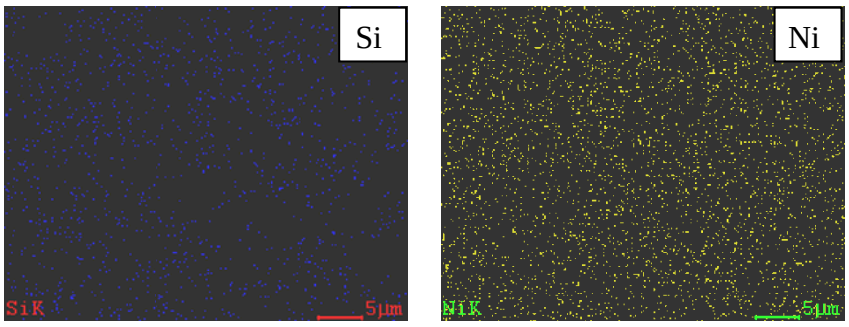

Figure 5.18 EDX mapping images of silicon (2 wt%) modification avicel supported nickel (20 wt%) catalyst

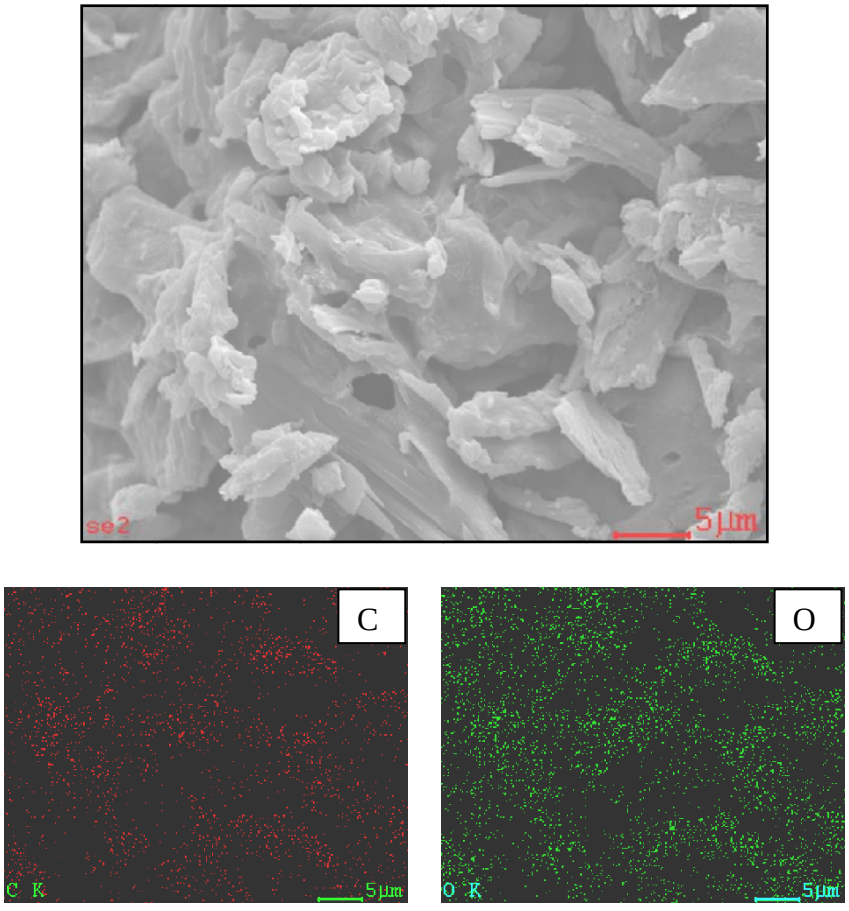

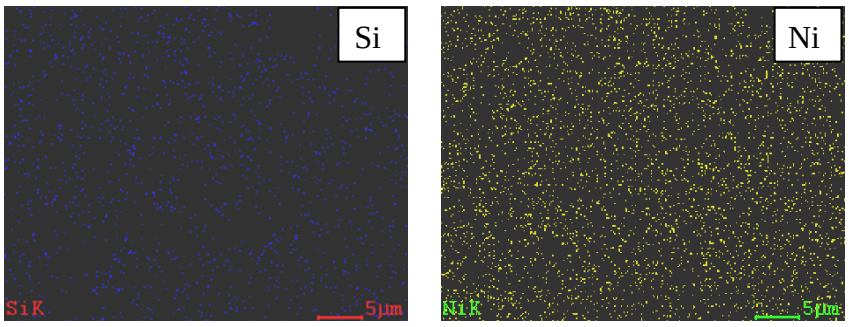

Figure 5.19 EDX mapping images of silicon (6 wt%) modification avicel supported nickel (20 wt%) catalyst

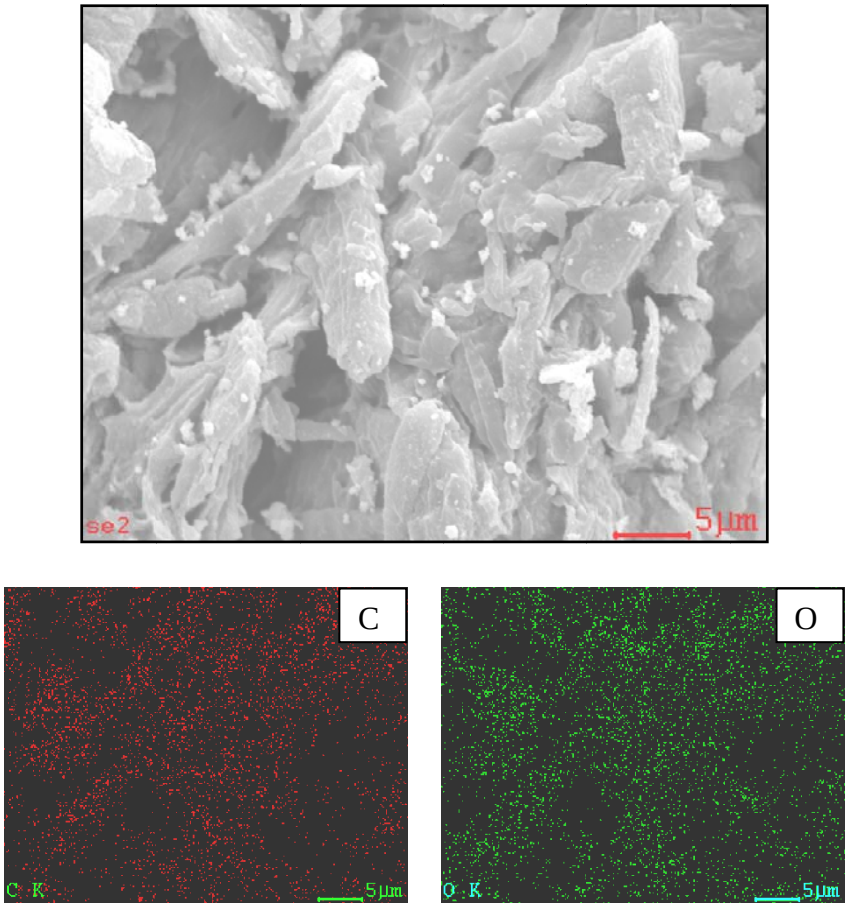

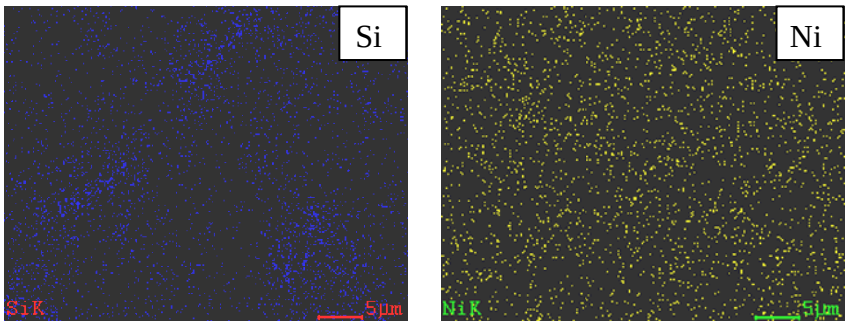

Figure 5.20 EDX mapping images of silicon (12 wt%) modification avicel supported nickel (20 wt%) catalyst

The compositions of samples are shown in weight percentage and atoms percentage, as seen in table 5.6. The results were displayed that the composition of samples were consisted of carbon, oxygen, silicon and nickel. The highest nickel on surface or 1-5µm depth was obtained at 57.94 wt% and 24.43 at% at 6 wt% of silicon.

Table 5.6 Determine composition of silicon modification avicel supported nickel by energy dispersive X-ray spectroscopy (EDX)

Samples	wt%				At%			
	C	O	Si	Ni	C	O	Si	Ni
Ni/AV-2Si	21.81	22.44	1.17	54.58	43.34	33.48	0.99	22.19
Ni/AV-6Si	21.56	19.62	0.87	57.94	44.44	30.36	0.77	24.43
Ni/AV-12Si	34.66	25.90	5.40	34.05	54.69	30.68	3.64	10.99

5.3.1.3 Phase analysis by X-ray diffraction (XRD)

XRD (Phase analysis by X-ray diffraction) was used to characterize the chemical composition of crystalline by repetitive arrangements of atoms which each element has own unique diffraction pattern. XRD methods for crystallite size determination are applicable to crystallites in the range of 2-100 nm. The diffraction peaks are very broad for crystallites below 2-3 nm, while for particles with size above 100 nm the peak broadening is too small. The samples were analyzed at diffraction angles between 20° to 80°. XRD patterns of various silicon modification avicel

supported nickel followed by calcined under air condition at 200°C, 1 atm for 4 hr were shown in Figure 5.21. From XRD images of silicon modification supported nickel loading 20 % by weight, all samples exhibited weak peaks at 2θ of 34.3° for avicel. The strongest diffraction peaks of SiO_2, which should be around 23.2°, can be observed in all samples. The diffraction peaks of Ni/AV-12Si at 2θ of 37.3, 43.4, 62.8° exhibited NiO and at 2θ of 44 and 52° displayed Ni on catalysts. [22-26]

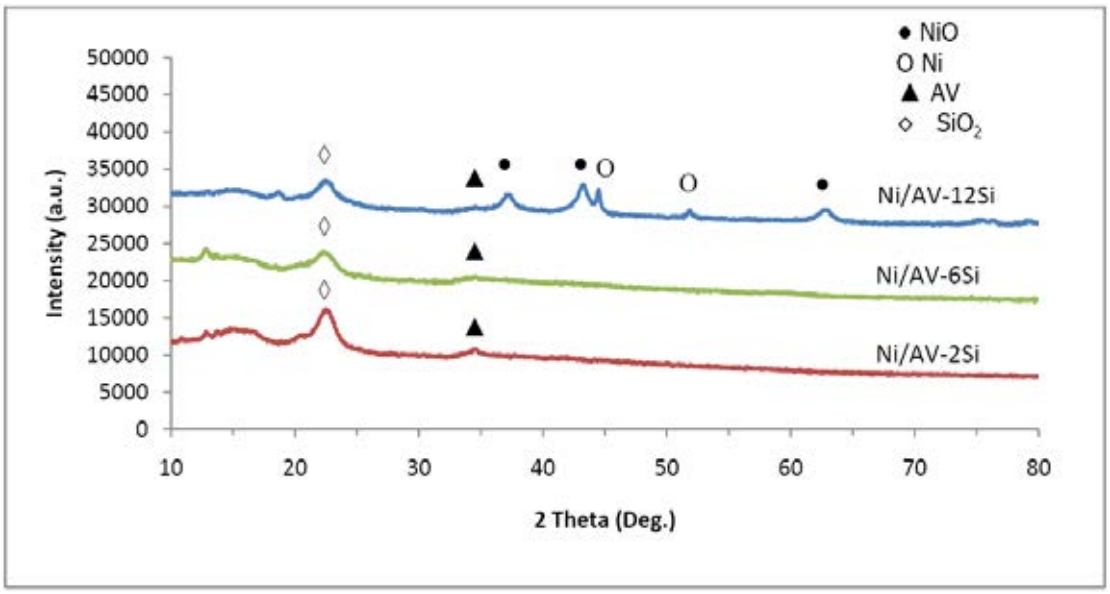

Figure 5.21 XRD patterns of silicon modification of cellulose supported nickel catalysts by silicon loading

5.3.1.4 N_2 Physisorption (BET specific surface areas determination)

Surface area of aluminium modification of cellulose supported nickel was determined by N_2 physisorption (BET). The results showed surface areas of Ni/AV-6Si, Ni/AV-12Si were 2.2256 and 3.3551 m^2/g, respectively. From the experiment, surface area was increased when increase silicon loading to the samples.

5.3.1.5 TGA (Thermal gravimetric analysis)

TGA (Thermal gravimetric analysis) is a very convenient method for evaluate the oxidation state of component by reduce or oxidize sample in controlled environment and measure the weight variation. The samples were examined at

temperature between 30-200°C. Figure 5.22 shows TGA profile of various silicon modification avicel supported nickel followed by calcined under air condition at 200°C, 1 atm for 4 hr. From Figure 5.22, the maximum weight loss of Ni/AV-2Si can be observed up to 9%. The lowest weight loss, which was belonging to Ni/AV-12Si, showed 4.5%. Weight loss of Ni/AV-6Si can be estimated to 7.5%. Thus, thermal stability of Ni/AV-12Si was satisfied more than Ni/AV-2Si and Ni/AV-6Si. From TGA profile of various alumina modification avicel supported nickel, moisture in sample was initially removed from 25°C to 100°C and organics parts were decomposed after 100°C. After 100°C organics parts were decomposed and nickel oxide was transformed to nickel.

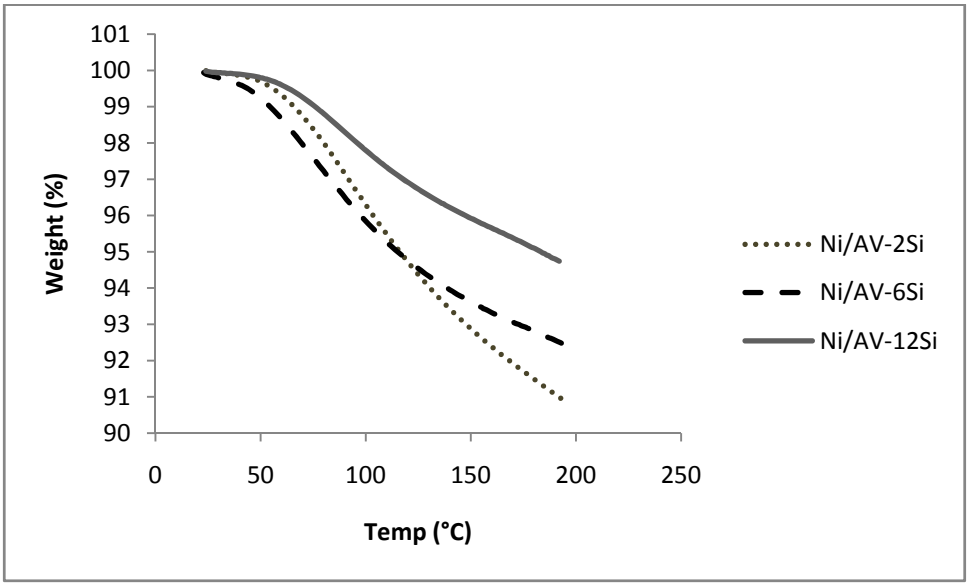

Figure 5.22 TGA analysis characterizing weight loss (%) of silicon modification of cellulose supported nickel catalysts

5.3.2 Catalyst activity

CO_2 hydrogenation was carried out in fixed bed reactor. The main product and by products in this experiment were methane and carbon dioxide, respectively. Sample (0.1 g) was packed in a fixed-bed microreactor. Sample was reduced by H_2 (50ml/min) at 220°C for 5 hr. to change nickel oxide to metal. Ar (8ml/min) and H_2 (22ml/min) was flew to reduce CO_2 before start reaction and record concentration of

CO_2 in feed by gas chromatography. CO_2 hydrogenation was carried out at 220°C and 1 atm. Steady state was reached in 5 hr. The sample from reactor was analyzed every 1 hr by gas chromatography to determine CO_2, CO and CH_4 composition. CO_2 conversions of silicon modification supported nickel at steady state were estimated to 6.29-35.87% and Ni/AV-6Si showed the highest CO_2 conversion. The selectivity to CH_4 was 64.19-39.83.57% and rate of reaction was 4.05-23.06 gCH_2/gcat.hr. By changing silicon loading, the highest selectivity to CH_4 was obtained at 2 wt% of silicon. The optimum silicon loading to reach the highest rate of reaction was 6 wt%. CO_2 conversion (%), selectivity (%) and rate of reaction were shown in table 5.7.

Table 5.7 Catalyst activity of silicon modification of cellulose supported nickel catalysts

Catalysts	CO_2 conversion (%)	Selectivity (%)		Rate of reaction
	Steady state	CH_4	CO	(gCH_2/gcat.hr)
Ni/AV-2Si	24.14	83.57	16.43	15.52
Ni/AV-6Si	35.87	64.19	35.81	23.06
Ni/AV-12Si	6.29	78.73	21.27	4.05

CHAPTER VI

CONCLUSIONS AND RECOMMENDATION

Conclusions and discussion are explained in this chapter. Conclusion of the effect of alumina and silicon modification of cellulose-supported nickel catalysts for CO_2 hydrogenation are described in section 6.1 and suggestion for study in the future is introduced in section 2.

6.1 Conclusions

1. Avicel was roughness shape and layer of amorphous structure, which the qualifications were suitable to use as a support catalyst. When nickel loading of 20 wt% was impregnated onto the support, surface areas of samples were increased. Surface area increased because the layers of nickel and nickel oxide covered on samples. After reaction test, Avicel supported nickel can be used as catalyst for CO_2 hydrogenation because of high selectivity, for CH_4.

2. The samples, which were composed of aluminium loadings of 2, 6, 12 wt% in avicel supported nickel, were investigated the to effect of CO_2 hydrogenation. Surface area tends to decrease when aluminium loading increases due to blockage pores on support from alumina. Alumina had less effect on thermal stabilities of samples as shown in TGA profile. The results demonstrated that conversion and rate of reaction were improved when using aluminium loading of 6 wt% impregnated on the support.

3. The samples, which were composed of silicon loadings of 2, 6, 12 wt% in avicel supported nickel, were investigated to the effect of CO_2 hydrogenation. The increase of silicon loading affected on increased surface area and thermal stabilities of catalysts. When silicon content reaches 6 wt%, CO_2 conversion and rate of reaction performed high performance. The highest selectivity can be observed with alumina loading of 2 wt%.

4. From the experiment, alumina loading greatly improves CO_2 conversion and rate of reaction. When alumina was impregnated on the support, CO_2 conversion and rate of reaction were distinctly high. The effect of silicon was important to improve selectivity and thermal stability.

6.2 Recommendation

Table 6.1 shows the summary of catalyst activity from this experiment. It can be seen that CO_2 conversions and rate of reactions were increased when using aluminium loading on the support. For silicon, it was greatly affected to improve selectivity and thermal stability.

Table 6.1 Catalyst activity of aluminium and silicon modification of cellulose supported nickel catalysts

Catalysts	CO_2 conversion (%)	Selectivity (%)		Rate of reaction
	Steady state	CH_4	CO	(gCH_2/gcat.hr)
Ni/AV	23.20	87.88	12.12	14.92
Ni/AV-2Al	72.41	31.98	68.02	46.55
Ni/AV-6Al	99.51	25.19	74.81	63.98
Ni/AV-12Al	95.35	39.87	60.13	61.30
Ni/AV-2Si	24.14	83.57	16.43	15.52
Ni/AV-6Si	35.87	64.19	35.81	23.06
Ni/AV-12Si	6.29	78.73	21.27	4.05

1. The combination of aluminium and silicon modification of cellulose supported nickel catalysts should be investigated.

2. The reuse of catalysts should be investigated.

3. CO chemisorption should be investigated to determine the number of reduced surface nickel metal atoms.

REFERENCES

[1] Di Li, Nobuyuki Ichikuni, Shogo Shimazu, and Takayoshi Uematsu, Catalytic properties of sprayed Ru/Al2O3 and promoter effects of alkali metals in CO_2 hydrogenation. Applied Catalysis A: General, 1998. 18(12): p. 351-358.

[2] Hitoshi Kusama, Kiyomi Okabe, Kazuhiro Sayama, and Hironori Arakawa, CO_2 hydrogenation to ethanol over promoted Rh/SiO_2 catalysts. Catalysis Today, 1996. 28(3): p. 261-266.

[3] Feg-Wen Chang, Maw-Suey Kuo, Ming-Tseh Tsay, and Ming-Chung Hsieh, Hydrogenation of CO_2 over nickel catalysts on rice husk ash-alumina prepared by incipient wetness impregnation. Applied Catalysis A: General, 2003. 247: p. 309-320.

[4] Rostrup-Nielsen, and Jens R., Industrial relevance of coking. Catalysis Today, 1997. 37: p. 225-232.

[5] Podczeck F., Knight P.E.F., and Newton J.M., The evaluation of modified microcrystalline cellulose for the preparation of pellets with high drug loading by extrusion/spheronization. Science Direct, 2008. 350(1-2): p. 145-54.

[6] Rubin, and E.M., Genomics of cellulosic biofuels. Nature, 2008. 454(7206): p. 841-5.

[7] Erhan Aksoylu, and Z. hsen Onsan, Hydrogenation of carbon oxides using coprecipitated and impregnated Ni/Al_2O_3 catalysts. Applied Catalysis A: General, 1997. 164: p. 1-11.

[8] Jianzhong Li, and G.L., Reaction performance of partial oxidation of methane over Ni/SiO_2 catalysts using monodisperse silica sol as supporting precursor. Applied Catalysis A: General, 2004. 273: p. 163-170.

[9] Masahisa Wada, R.H., Ung-Jin Kimb, and Sono Sasaki, X-ray diffraction study on the thermal expansion behavior of cellulose Ib and its high-temperature phase. Polymer Degradation and Stability, 2010. 95: p. 1330-1334.

[10] Yoshiharu Nishiyama, P.L., and Henri Chanzy, Crystal Structure and Hydrogen-Bonding System in Cellulose IB from Synchrotron X-ray and Neutron Fiber Diffraction. JACS articles, 2002.

[11] Diane R. Milburn, K.V.R.C., Robert J. O'Brien, and Burtron H. Davis, Promoted iron Fischer-Tropsch catalysts: characterization by thermal analysis. Applied Catalysis A: General, 1996. 144: p. 133-146.

[12] Yinyong Suna, and others, Improved catalytic activity and stability of mesostructured sulfated zirconia by Al promoter. Applied Catalysis A: General, 2004. 268: p. 17-24.

[13] Wenjuan Houa, and others, Effect of SiO_2 content on iron-based catalysts for slurry Fischer–Tropsch synthesis. Fuel Processing Technology, 2008. 89: p. 284-291.

14] Das K.K., and S.N., Nickel, its adverse health effects & oxidative stress. Indian J Med Res, 2008. 128: p. 412-425.

[15] A. Slagtern, Y.S., C. Leclercq, X. Verykios, and C. Mirodatos, Specific Features Concerning the Mechanism of Methane Reforming by Carbon Dioxide over Ni/La_2O_3 Catalyst. Journal of Catalysis, 1997. 172: p. 118-126.

[16] Li-Hui Ren, H.-L.Z., An-Hui Lu, Yan Hao, and Wen-Cui Li, Porous silica as supports for controlled fabrication of $AuCeO_2SiO_2$ catalysts for CO oxidation Influence of the silica nanostructures. Microporous and Mesoporous Materials, 2012. 158: p. 7-12.

[17] Bnra N.J., and othres, MELANOPHLOGITE, A CUBIC POLYNIORPH OF SILICA. THE AMERICAN MINERAIOGIST, 1963. 48.

[18] Musila J., and others, Thermal stability of alumina thin films containing Gamma-Al_2O_3 phase prepared by reactive magnetron sputtering. Applied Surface Science, 2010. 257: p. 1058-1062.

[19] Susuki T., Y.M., T. Hiraj, and S. Hayashi, Preliminary attempt to enhance the hydrogenation of carbon dioxide to methane on cobalt oxide catalyst by adding $CuO-ZnO-Cr_2O_3$. International Journal of Hydrogen Energy, 1993. 18(12): p. 979-983.

[20] Schumacher C., and others, Trends in low-temperature water-gas shift reactivity on transition metals. Journal of Catalysis, 2005. 229(2): p. 265-275.

[21] Bayat, M., M.R. Rahimpour, and B. Moghtaderi, Genetic algorithm strategy (GA) for optimization of a novel dual-stage slurry bubble column membrane configuration for Fischer–Tropsch synthesis in gas to liquid (GTL) technology. Journal of Natural Gas Science and Engineering, 2011. 3(4): p. 555-570.

[22] Yoshifumi Horita, T.Y., Seichi Rengakuji, and Y. Nakamura, Preparation and Characterization of Al_2O_3 Thin Films from Liquid Phase.

[23] Zhong LI, and T.S.a.L.G., Preparation and morphology of porous SiO_2 ceramics derived from fir flour templates. Journal of the Serbian Chemical Society, 2010: p. 385-394.

[24] Prabhu B., C.S., L. Ana,b, and R. Vaidyanathan, Synthesis and characterization of high volume fraction Al–Al_2O_3 nanocomposite powders by high-energy milling. Materials science&engineering, 2006: p. 192-200.

[25] Hui Chen, M.X., Shenghua Hu, and Jianyi Shen, The effect of surface acidic and basic properties on the hydrogenation of lauronitrile over the supported nickel catalysts. Chemical Engineering Journal, 2012: p. 677-684.

[26] Yongju Bang, S.J.H., Jeong Gil Seo, Min Hye Youn, Ji Hwan Song, and I.K. Song, Hydrogen production by steam reforming of liquefied natural gas (LNG) over ordered mesoporous nickelealumina catalyst. Hydrogen energy, 2012: p. 17967-17977.

APPENDICES

APPENDIX A

CALCULATION FOR CATALYST PREPARATION

Calculation of aluminium modification on support

Aluminium loading of 2, 6 and 12 wt% modification on Avicel was prepared by impregnation method, the calculations are shown:

Reagent: -Aluminium(III) nitrate 99% [$Al(NO_3)_3$]

Molecular weight of $Al(NO_3)_3$: 375.13 g/mol

Atomic weight of Al: 26.9815 g/mol

-Support: Avicel

Al loading of 2 wt% calculation as shown:

Support 98 g required Al 2 g

Support 1.3 g required Al = (2 x 1.3)/98

= 0.0265 g

Al 26.9815 g from $Al(NO_3)_3$= 375.13 x 0.99 g

Al 0.0265 g from $Al(NO_3)_3$= (375.13 x 0.99 x 0.0265) / 26.9815

= 0.3648 g

Calculation of silicon modification on support

Si loading of 2, 6 and 12 wt% modification on Avicel was prepared by impregnation method, the calculations are shown:

Reagent: Tetraethyl Orthosilicate 98% [$Si(OC_2H_5)_4$]

Molecular weight of TEOS: 208.33 g/mol

Atomic weight of Si: 28.0855 g/mol

-Support: Avicel

Si loading of 2 wt% calculation as shown:

Support 98 g required Si 2 g

Support 1.3 g required Si = (2 x 1.3)/98

= 0.0265 g

Si 28.0855 g from TEOS = 208.33 x 0.98 g

Si 0.0265 g from TEOS = (208.33 x 0.98 x 0.0265) / 28.0855

= 0.1926 g

Calculation of Al and Si modification of cellulose-supported nickel catalyst

Al modification of cellulose-supported nickel catalyst was prepared by impregnation method, the calculations are shown:

Reagent: Nickel(II) nitrate hexahydrate [$Ni(NO_3)_2 \cdot 6H_2O$]

Molecular weight of $Ni(NO_3)_2 \cdot 6H_2O$: 290.79 g/mol

Atomic weight of Ni: 58.6934 g/mol

-Support: Avicel

Al (2 wt%) modification of cellulose-supported nickel (20 wt%) catalyst calculation as shown:

Support and promoter (Al) 80 g required Ni 20 g

Support and promoter (Al) 1.0054 g required Ni = (20 x 1.0054)/80

= 0.2514 g

Ni 58.6934 g required $Ni(NO_3)_2 \cdot 6H_2O$ 290.79 g

Ni 0.2514 g required $Ni(NO_3)_2 \cdot 6H_2O$ = (290.79 x 0.2514)/58.6934 g

= 1.2455 g

Si (2 wt%) modification of cellulose-supported nickel (20 wt%) catalyst calculation as shown:

Support and promoter (Si) 80 g required Ni 20 g

Support and promoter (Si) 0.8716 g required Ni = (20 x 0.8716)/80

= 0.2177 g

Ni 58.6934 g required $Ni(NO_3)_2 \cdot 6H_2O$ 290.79 g

Ni 0.2177 g required $Ni(NO_3)_2 \cdot 6H_2O$ = (290.79 x 0.2177)/58.6934 g

= 1.0786 g

APPENDIX B

CALCULATION OF CO_2 CONVERSION, REACTION RATE AND SELECTIVITY

CO_2 conversion was determined by the following equation:

$$CO_2 \text{ conversion (\%)} = \frac{100 \times [mole of\ CO_2\ in\ feed - mole of\ CO_2\ in\ product]}{mole of\ CO_2\ in\ feed}$$

Reaction rate was calculated from CO_2 conversion as follows:

Let the weight of catalyst used	=	W	g
Flow rate of CO_2	=	2	cc/min
Reaction time	=	60	min
Weight of CH_2	=	14	g
Volume of 1 mole of gas at 1 atm	=	22400	cc/mol

Reaction rate (g CH_2/g of catalyst.h)

$$\text{Reaction rate} = \frac{\%\ CO_2 \text{ conversion} \times \text{feed flow rate of } CO_2 (\text{cm}^3/\text{min}) - \text{ mole of } CH_2 (\text{g/mol})}{\text{catalyst weight (g)} \times 22{,}400\ (\text{cm}^3/\text{mol})}$$

Selectivity of B was calculated by the following equation:

$$\text{Selectivity of B (\%)} = 100 \times [mole\ of\ B\ formed / mole\ of\ total\ products]$$

B is product, which mole of B was determined by calibration curve of products.

VITA

Ms. Nattakan Jungjittamat was born on September 25th, 1985 in Thailand. She graduated bachelor's degree from Mahidol University in the faculty of Chemical Engineering in 2007. After that, she studied master's degree at Chulalongkorn University, faculty of Chemical Engineering in 2010.